Advances in Water Resources 112 (2018) 124–146

Contents lists available at ScienceDirect

Advances in Water Resources

journal homepage: www.elsevier.com/locate/advwatres

Hydrologic responses to restored wildfire regimes revealed by soil moisture-vegetation relationships

Gabrielle Boisramé[*,a], Sally Thompson[b], Scott Stephens[a]

[a] Department of Environmental Science, Policy, and Management, UC Berkeley, Berkeley, CA, 94720, USA
[b] Department of Civil and Environmental Engineering, UC Berkeley, Berkeley, CA, 94720, USA

ARTICLE INFO

Keywords:
Wildfire
Mixed conifer
Wetland
Shrub
Sierra Nevada
Soil moisture

ABSTRACT

Many forested mountain watersheds worldwide evolved with frequent fire, which Twentieth Century fire suppression activities eliminated, resulting in unnaturally dense forests with high water demand. Restoration of pre-suppression forest composition and structure through a variety of management activities could improve forest resilience and water yields. This study explores the potential for “managed wildfire”, whereby naturally ignited fires are allowed to burn, to alter the water balance. Interest in this type of managed wildfire is increasing, yet its long-term effects on water balance are uncertain. We use soil moisture as a spatially-distributed hydrologic indicator to assess the influence of vegetation, fire history and landscape position on water availability in the Illilouette Creek Basin in Yosemite National Park.

Over 6000 manual surface soil moisture measurements were made over a period of three years, and supplemented with continuous soil moisture measurements over the top 1m of soil in three sites. Random forest and linear mixed effects models showed a dominant effect of vegetation type and history of vegetation change on measured soil moisture. Contemporary and historical vegetation maps were used to upscale the soil moisture observations to the basin and infer soil moisture under fire-suppressed conditions. Little change in basin-averaged soil moisture was inferred due to managed wildfire, but the results indicated that large localized increases in soil moisture had occurred, which could have important impacts on local ecology or downstream flows.

1. Introduction

The importance of forested montane watersheds for water supply in many regions worldwide has long raised the question of whether forest management could be used to enhance water yields (Baker, 1986; Hawthorne et al., 2013; Hibbert, 1965; Kattelmann et al., 1983; Lesch and Scott, 1997; Troendle, 1983). More recently, the potential for such management actions to improve forest health and productivity in fire-suppressed forests has raised the prospect of a “win-win” scenario for ecology and water supply. Fire suppression has led to unnaturally dense forests in many parts of the world, including California’s Sierra Nevada (Collins et al., 2011; McIntyre et al., 2015). Forest management that reduces tree density could increase growth rates of the remaining trees (Bréda et al., 1995; Ruprecht and Stoneman, 1993), reduce competition between trees for scarce resources (Grant et al., 2013), and reduce the potential for catastrophic wildfire (Aust and Blinn, 2004; Kauffman, 2004; Pollet and Omi, 2002), thus improving forest resilience. In turn, reduced water demand in thinned forests can result in higher water availability downstream, and increasing non-forested wetland area can increase a watershed’s capacity for water storage (Dubé et al., 1995; Fletcher et al., 2014). Soil moisture is a hydrologic variable that integrates all of these processes, as subsurface stores provide a source of water for both vegetation needs and streamflow generation, and changing soil moisture reflects changes in local water balance.

The hydrologic impacts of forest management practices are highly uncertain; scientific studies are limited and have mixed results. For example, observed flow increases following forest thinning range from as little as 1% to 70% (Kattelmann et al., 1983; Lesch and Scott, 1997). Differences in outcome appear to depend on many factors including the specifics of the forest treatment, local topography, vegetation type, and weather (Baker, 1986; Hawthorne et al., 2013). Problematically, increases in water yield typically persist for only ≈ 5 years following forest treatments (Brown et al., 2005), suggesting that frequent re-treatment would be needed to sustain water supply benefits. Such high frequencies may impose important feasibility constraints on the implementation of labor-intensive management efforts. Conventional forest management practices such as thinning, clearing, or prescribed fire, may also be difficult to upscale to the point where they can have

* Corresponding author.
E-mail address: gboisrame@berkeley.edu (G. Boisramé).

https://doi.org/10.1016/j.advwatres.2017.12.009
Received 1 May 2017; Received in revised form 8 December 2017; Accepted 8 December 2017
Available online 09 December 2017

meaningful impacts on water resources. Thus, identifying alternative and scalable forest management strategies would be attractive.

Managed wildfire may offer such an approach. Under this management strategy, naturally ignited fires are allowed to burn, provided a fire management plan is identified and clear conditions for fire operations are in place (e.g. to prevent air quality impacts or protect sensitive areas). The fire-return interval in many fire-prone mountain watersheds is relatively short (e.g. ≈ 7–15 years in the mid-pine belt in the Sierra Nevada, Collins and Stephens, 2007), meaning that this approach can alter the understory and ground litter (Collins et al., 2016; Stephens et al., 2009), reduce forest density and leaf area (Kane et al., 2014), and replace land cover (Boisramé et al., 2017a) on timescales commensurate with those of hydrologic recovery from such disturbance.

Managed wildfire policies have been implemented long-term in only a few watersheds. In these locations, they are associated with large-scale reductions in forest cover and density over multi-decadal timescales (Boisramé et al., 2017b; Kane et al., 2014). These changes may have reduced the extent of severe fires (Collins and Stephens, 2007), lowered drought-induced forest mortality relative to neighboring basins (Boisramé et al., 2017a), and increased the biodiversity of pollinating insects (Ponisio et al., 2016). These positive outcomes support the potential for managed wildfire to mimic some of the landscape-scale benefits of thinning or patch-felling at large scales and at relatively frequent intervals, without requiring mechanized harvest and the associated costs, labor, and soil disturbance. To date, however, the hydrologic impacts of managed wildfire are poorly understood. The basins with long-term managed wildfire regimes lack long term stream gauges and baseline (i.e. pre-treatment) hydrologic measurements. The study watershed considered here, the Illilouette Creek Basin (ICB), is gauged after its confluence with the larger Upper Merced River. While there may be a small signal of enhanced streamflow production at this gauge following the institution of the managed wildfire regime in the ICB in 1972 (Boisramé et al., 2017a), analysis of flow trends offers little insight into the effects of the fire regime on basin hydrology (both due to uncertainty caused by high interannual variability in flows, and the basin-aggregated nature of streamflow). Soil moisture provides a useful metric for observing sub-watershed scale hydrology, representing the local balance between precipitation, deep drainage, evapotranspiration, and discharge.

Soil moisture dynamics in a burned watershed are altered by a complex suite of hydrologically relevant processes initiated by wildfire (Brown et al., 2005). For instance, burning can have counteractive effects on the amount and timing of snowmelt inputs to groundwater stores: blackened trees provide a source of long-wave radiation, and canopy losses reduce shading, speeding melting and sublimation rates (Neary et al., 2005; Tague and Dugger, 2010), but canopy losses also reduce interception and can reduce long-wave radiation, enhancing snowpack accumulation and delaying snowmelt compared to dense forest (Ellis et al., 2013; Lundquist et al., 2013). Similarly, although loss of mature trees can reduce transpiration (Bréda et al., 1995; He et al., 2013; Ma et al., 2010; Rambo and North, 2009; Zhang et al., 2001), loss of shading can increase soil evaporation (Biederman et al., 2014) while regrowth of understory vegetation or young life-stages can increase water demand, reducing soil moisture levels (Lane et al., 2010; Neary et al., 2005; Tague and Dugger, 2010; Vertessy et al., 1995; 2001). Most literature regarding fire-effects on watershed hydrologic balance focuses on large individual fires (Helvey, 1980; Langford, 1976, e.g.), or individual clearing/thinning treatments (Brown et al., 2005), rather than the long-term effects of cumulative vegetation change. Thus, the net hydrologic impact of managed wildfire over many decades and at basin scales remains uncertain.

The Illilouette Creek Basin is one of two basins in California (four in the western United States) where a managed wildfire regime has been in place for multiple decades. It holds wilderness status, meaning that soil and surface hydrology are relatively undisturbed by humans. Although no direct observations of change in the basin hydrology during the institution of the managed wildfire regime are available (there are no data for soil moisture, streamflow, or weather within the ICB dating from its fire suppressed state), fire effects on vegetation cover in the ICB have been reconstructed from air photo records (Boisramé et al., 2017b). These reconstructions show that between 1970 (when the basin was still fire-suppressed) and 2012 the watershed lost 24% of its conifer cover, while dense meadow area increased by 155%, shrub area by 35%, and sparse meadow area by 199% (Boisramé et al., 2017b).

The type of vegetation growing at a location is frequently correlated with local hydrological conditions (e.g. Araya et al., 2011; Milledge et al., 2013; Mountford and Chapman, 1993). For example, lodgepole pine (*Pinus contorta*, PICO), a common species in ICB, establishes in intermediately wet areas of meadows (Helms and Ratliff, 1987), while whitethorn ceanothus (*Ceanothus cordulatus*) grows in exposed, dry sites (Fites-Kaufman et al., 2007). Within the ICB, Kane et al. (2015) found relationships between water balance and forest structure, suggesting that vegetation observations can be related to water availability, and the history of vegetation change in the basin could therefore provide a proxy history of hydrologic changes. In this study we use soil moisture to represent these hydrologic changes, since it integrates shallow hydrologic fluxes and therefore is a useful spatially-explicit indicator of water budget partitioning. Reconstructing hydrologic change (as represented by changing soil moisture) using vegetation is undoubtedly an approximate method, but it overcomes major limitations of other approaches such as remote sensing of soil-moisture related indices (Musick and Pelletier, 1988), which are precluded in areas with dense vegetation cover (Crist and Cicone, 1984), and thus cannot be used to examine the effects of transitions from forested to unforested sites.

This study aims to identify the effect of the changing fire regime on water availability in the ICB by measuring surface soil moisture, establishing its dependence on vegetation, fire history and topography, and using these relationships to extrapolate soil moisture observations to the basin scale under contemporary and historic vegetation distributions. Differences in these basin-scale soil moisture surfaces would then provide an estimate of the change in soil moisture following the change in fire management. In order to justify this modeling approach, we first answer the following questions:

- Is surface soil moisture a useful indicator of ecologically-relevant water storage (as might be influenced by, or might influence, local vegetation)?
- Is vegetation a useful indicator of surface soil moisture values?
- Under a given vegetation type, can topography and fire history explain spatial variations in soil moisture?

Ideally, we would estimate total soil water storage using continuous moisture measurements over the depth of the soil profile at many locations. This would give the most complete measure of the balance between precipitation, evapotranspiration, and runoff. However, wilderness regulations (U.S. Congress, 1964) limited such observations (which require disturbance of the soil profile and installation of temporary instrumentation) to three sites in the ICB. Therefore we relied primarily on spatially extensive but shallow (top 12 cm) soil moisture measurements (> 6000 in 90 sites) made twice annually over three consecutive growing seasons (2014 through 2016). Although surface soil moisture cannot be directly extrapolated to subsurface water storage, it is often closely related to water table depth (Sörensen et al., 2006) and plant available water (Gonzalez-Zamora et al., 2016). All observations were made during drought years of varying characteristics and severity (from extreme drought in 2014–2015 to near-normal winter precipitation in 2015–2016) and therefore do not necessarily apply to wet years. The observations were made at least nine years after the most recent large fire in the ICB and do not capture short-term post-

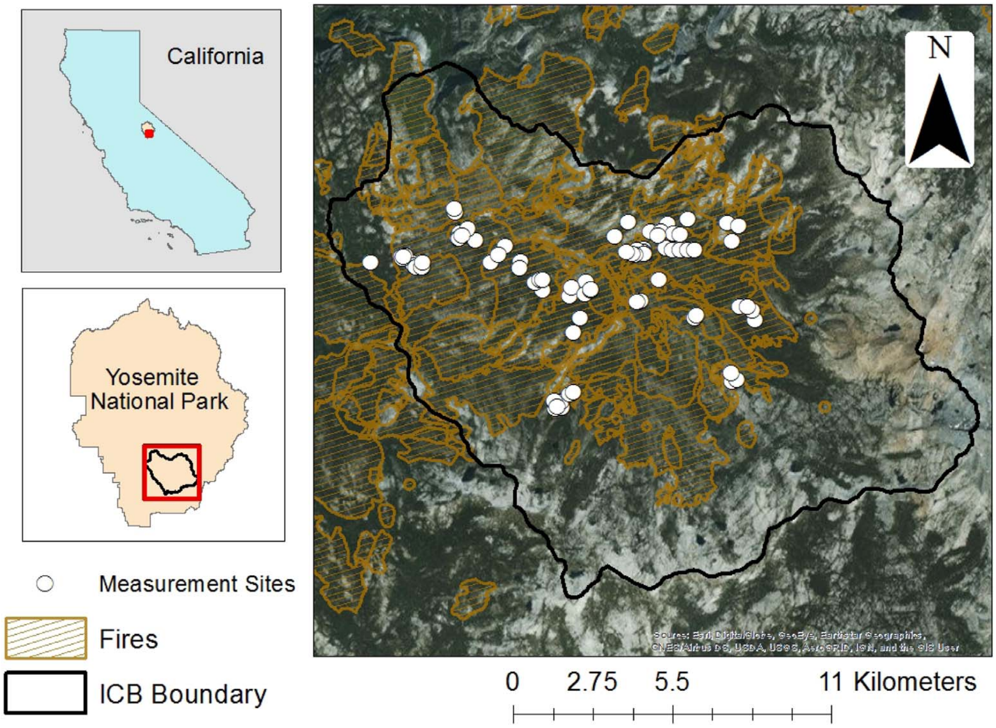

Fig. 1. Locations of soil moisture measurement sites and all fires since 1970. Imagery source: Esri.

fire soil moisture responses.

2. Materials and Methods

2.1. Study Site

The Illilouette Creek Basin (ICB) is a 150 km^2 basin within the Upper Merced Watershed in Yosemite National Park, California, USA (Fig. 1), spanning an 1800 m to ≈ 3000 m elevation range in the central Sierra Nevada. This area experiences a Mediterranean-type climate, with average January daily minimum temperatures ranging from − 5°C to 1°C, and average July daily maximum temperatures of ≈ 25°C (2000–2015; http://www.wrcc.dri.edu ; stations: White Wolf, Crane Flat). Average annual precipitation (Oct-Sep) ranged from 47 to 60 cm (2000-2015), dominated by winter snow. The basin is covered by coniferous forests (dominated by Jeffrey pine, *Pinus jeffreyi*, red fir, *Abies magnifica*, white fir, *Abies concolor*, and *P. contorta*), granite outcrops, meadows and shrublands (dominated by whitethorn ceanothus, *C. cordulatus*) (Collins et al., 2007). The area never experienced timber harvesting and likely had minimal impacts from livestock grazing (Collins and Stephens, 2007).

Fire suppression began in the ICB in the late 19th century, at a time when fire suppression was becoming common practice in many U.S. forests (Collins and Stephens, 2007), and the total area burned between 1880 and 1973 was only 0.08 km^2. In 1972 the ICB transitioned to a managed wildfire policy (van Wagtendonk, 2007), resulting in a new fire regime with very similar fire frequency and extent to those inferred by tree ring analysis from the pre-suppression period (contemporary mean fire return intervals are 6.8 years, compared to a 6.3 year mean from 1700 to 1900) (Collins and Stephens, 2007). During the managed wildfire period, 30 fires exceeding 40 ha extent burned in the ICB, forming a mosaic of vegetation change, where high severity burn patches intermix with intact forests (Collins and Stephens, 2010, Fig. 2), and leading to a large range in time-since-last-fire and vegetation condition across the basin. Seventy-five percent of the vegetated area, and 52% of the total basin area have burned since 1972.

Fig. 2. Photo of a burned study site. Dense shade-intolerant and drought-intolerant understory is growing in a burned area that was once densely forested, adjacent to an intact mature upper montane mixed conifer forest.

2.2. Field measurements

Surface soil moisture was mapped in the ICB in the summers of 2014–2016. A total of 6220 measurements were made in 90 sites, covering representative combinations of burn severity, time since fire, slope, aspect, elevation, and vegetation cover (Fig. 1, Table A.1). Thirty-seven sites were selected to overlap with established research plots (Collins et al., 2016). Fifty-three new sites were selected to represent combinations of slope, aspect, burn severity, and vegetation cover omitted in the previous plots. Locations for most of these new sites were selected by identifying desired combinations of traits in ArcGIS (http://www.arcgis.com), constraining locations to those accessible by foot, and sampling randomly within the identified areas;

twelve of the new locations were chosen opportunistically once in the field.

The volumetric water content (VWC) of soils was measured by inserting a 12 cm time-domain reflectomer (TDR) Hydrosense II probe vertically into the surface soils, having first removed leaf litter or duff. Given the high degree of homogeneity amongst the granitic loamy sands in the ICB a mineral-soil calibration, which typically has a 3% accuracy (Campbell Scientific, 2015), was used for all sites, in common with other large-scale surface soil moisture studies (e.g. Famiglietti et al., 2008). The TDR measurements for all sites gave reasonable values compared to qualitative estimates of soil moisture based on feel and appearance of the soil. Some organic wetland soils are present in the basin. Although the TDR was not recalibrated for these soils, maximum errors in VWC associated with TDR measurements in organic soils are reported as 0.05 (Roth et al., 1992), much smaller than typical differences in moisture between wetland and mineral soil sites. Consistency of measurements between handheld instruments was verified throughout the 3 field seasons. Handheld instruments were also verified against the continuously measuring TDRs from three vertical arrays (see below).

Soil moisture was measured at each site one to six times during early and late summer (when possible). Early summer measurements were made between May 21 and June 17 and late summer measurements between July 17 and August 9. Fifty-five sites were measured at least twice (e.g. early and late summer measurements in one year), 27 sites were measured at least four times, and seven sites were measured six times (both early and late summer measurements in all three years). Sites with highly variable soil moisture through time were high priorities for multiple measurements. Conversely, only a subset of sites exhibiting very dry early summer soil moisture (e.g. VWC ≤ 0.05) were re-measured in late summer, under the rationale that moisture conditions would remain similar across the dry summer months. We avoided taking measurements during or immediately following heavy rainfall, though a small number of measurements did occur within one day of precipitation. Both our continuously measuring soil moisture sensors (see below) and a subset of manual measurements taken before and after rainfall verified that individual summer storms affected surface soil moisture by a negligible amount compared to seasonal changes.

In most sites 30 evenly spaced soil moisture measurements (25 for repeat measures in homogeneous sites) were made within a 30m by 30m grid. Additional measurements were made in heterogeneous sites. One meter spaced measurements were made across a 30 m transect in sites with obvious strong gradients in soil moisture (e.g. wetland sites bordered by dry uplands). The standard error of the per-site mean VWC (over 25–30 measurements) averaged 0.01 (max of 0.07). Standard errors were $\leq 10\%$ of the mean in 56% of sites and $\leq 20\%$ of the mean in 90% of sites.

At each site, dominant vegetation cover (to species level when possible), slope, aspect, and the presence of burned snags or fire scarred trees were recorded. Sites were georeferenced using handheld Garmin GPSMAP 62st and 64st devices (horizontal accuracy 3–10 m). Latitude and longitude were assigned to each measurement point based on location within the grid or transect. Locations were verified in ArcMap.

2.3. Relating surface and root-zone soil moisture

Under dry climatic conditions, shallow soil moisture can become decoupled from water availability across the soil column (Grayson et al., 1997; He et al., 2013), which could confound both associations with vegetation, and interpretation of shallow soil moisture patterns in terms of basin hydrology. To establish relationships between shallow soil moisture and whole-column water availability, TDR measurements were compared to two independent metrics of subsurface water content: (i) pre-dawn leaf water potentials, and (ii) three continuously reporting vertical soil moisture TDR arrays spanning the top 1m of soil.

2.3.1. Pre-dawn leaf water potential measurements

Pre-dawn measurements of leaf water potential provide a proxy for root-zone water availability, under the assumption that non-transpiring plants reached hydraulic equilibrium with soil water potential overnight (Bréda et al., 1995; Dawson et al., 2007). Leaf water potential was measured with a PMS 1505D pressure chamber (http://www.pmsinstrument.com/), following the methods of Dawson and Ehleringer (1993).

Pre-dawn leaf water potential was measured in whitethorn ceanothus, willow (multiple unidentified *Salix* species), lodgepole pine, Jeffrey pine, and aspen (*Populus tremuloides*) at five sites co-located with TDR measurements. At least three individuals were measured per species per site, and each site was measured in early and late summer. These water potentials were then compared to surface soil moisture measurements.

2.3.2. Vertical TDR arrays

Weather stations, including TDRs installed horizontally at $\approx$ 12 cm, 60 cm and 1m beneath the soil surface (12 cm CS655 Campbell Scientific Soil Water Content Reflectometers, TDRs, http://www.campbellsci.com), were installed in July 2015, in loamy sand soils beneath different canopy types (closed canopy, post-fire shrub, and post-fire wetland) occurring within 200 m of each other (See Appendix C for details). TDRs were installed horizontally into undisturbed soil and the access holes backfilled and compacted. Exact TDR depths vary slightly at each location due to reaching rock or the water table before 1 m, but the soil was ≥ 90 cm deep at all three locations. The TDRs record soil moisture every 10 minutes, and enable continuous comparison of surface soil moisture to depth-integrated water storage.

2.4. Spatial data

Topography, vegetation cover, and fire history were mapped for the ICB using ArcGIS (http://www.arcgis.com). Site characteristics were extracted from these maps. Topographic covariates (slope, aspect, elevation, distance to nearest stream, and upslope area) were derived from a LiDAR elevation map of the ICB, coarsened to 10 m^2 resolution from the original 1 m^2 map (Kane et al., 2015). Several specific topographic indices were computed:

- The *aspect index* was used to control for the influence of slope orientation on incident solar radiation. Rather than describing orientation according to compass direction, the aspect index transforms orientation to a 0–1 scale (south facing slopes ≈ 1 and north facing ≈ 0), as $0.5(1 - cos(Aspect - 30))$ (Kane et al., 2015).
- The *Topographic Wetness Index* (TWI) accounts for how topography may predispose a site to saturation via shallow subsurface flow. TWI is computed as $ln\frac{a}{tan(s)}$, where a is the upslope contributing area and s the local slope. The higher the TWI, the greater the topographic potential for saturation (Beven, 1983).
- The *Topographic Position Index* describes whether a site is in a valley ($TPI < 0$), a ridge ($TPI > 0$) or on a near-planar slope ($TPI \approx 0$). It is computed as

$$TPI = int((elev - focalmean(elev, annulus, 150, 300)) + .5)$$

where *elev* is the point's elevation in meters, *focalmean* is a function which takes the mean elevation over a ring surrounding the point with inner diameter of 150m and outer diameter of 300 m, and *int* refers to rounding the results to the nearest integer value (Weiss, 2001).

The ranges for all topographic and fire history values are given in Table A.1.

Dominant vegetation cover in 1969/1970 at the end of the fire suppressed period, and in 2012 following 40 years of managed wildfire, was mapped from aerial imagery (Boisramé et al., 2017b). Vegetation was classified as sparse meadow, dense meadow, shrub, aspen, and conifer. Dense meadows include wetlands and areas of dense herbaceous cover, which cannot be reliably separated using imagery. Sparse meadows include sparse shrub and/or herbaceous cover, and are dominated by bare ground. Exposed bedrock and talus fields were excluded from our analyses. These vegetation classifications were used for contemporary analysis, upscaling and extrapolation to historical maps.

Separately, the observed dominance of lodgepole pine (PICO) at a measurement site was considered an additional classifier for the contemporary analysis. While PICO could not reliably be identified separately from other conifer forest in aerial images, it is often associated with wet conditions relative to other conifers, and could thus be a useful indicator of hydrologic condition in the contemporary watershed.

Time since fire and times burned (since 1930) were computed from a digital fire atlas containing all recorded fire perimeters within Yosemite National Park (available from irma.nps.gov/Portal). If no fires occurred, time since fire was set to 100 years. Fire severity was calculated using a relative version of the differenced Normalized Burn Ratio (RdNBR), derived from Landsat Thematic Mapper images (Boisramé et al., 2017a; Collins et al., 2009). Thresholds for RdNBR fire severity classes (unchanged, low, moderate, and high) were taken from Miller and Thode (2007).

Spatial covariates were extracted from the spatial datasets for each subsite using ArcMap, and compared to field notes to verify accuracy. They were used in initial exploratory comparisons of soil moisture variability, as well as co-variates in the statistical models.

2.5. Other data

Weather data are incompletely observed across the ICB and throughout the Sierra Nevada generally. Thus, variability in weather conditions (and potentially other unobserved, time-varying drivers of VWC variability) was accounted for by using the year of measurement as a covariate in the statistical models of surface soil moisture described below. For example, 2015 had three times more summer precipitation than the other two years (120 mm in May–September, Yosemite Southern Entrance Station, http://www.ncdc.noaa.gov), while 2016 had the most winter precipitation (890 mm in the winter of 2015/2016 compared to < 400 mm the previous two winters). We were unable to improve model results by incorporating observations from nearby weather stations directly.

Prior to analysis, all covariates were tested to detect collinearity. No correlation between covariates exceeded $|r| > 0.7$, a common cutoff used to indicate unacceptable levels of collinearity (Dormann et al., 2013; Shmueli, 2010). Test models were run incorporating latitude and longitude as spatial predictors, but these covariates showed both high collinearity with other covariates and low significance and were dropped from the final models. For more details, see Appendix D.

2.6. Analysis of soil moisture variability

Soil moisture was related to site characteristics with statistical models trained on measured surface soil moisture. All models were fit using R software (http://www.r-project.org). Prior to model fitting, data were manipulated to create a dataset in which predictor and explanatory variables were resolved at similar spatial scales, and potential biases due to higher sampling frequency of certain sites were addressed as described below.

First, because the spatial predictor data are available at scales of 10 m–30 m, VWC measurements in each site were aggregated to the mean value under each dominant vegetation type within the site. This coarsening reduces the influence of fine-scale variations in, for example, microtopography, which are not captured by the covariates. The vegetation patch averaged data within individual sites are referred to as “subsites”. The subsite data formed the basis for all modeling.

Secondly, the prioritization of highly time-varying sites when sampling (as described in Section 2.2) meant that saturated sites in early summer and dry sites in late summer were under-represented in the data set. We used a gap-filling algorithm to correct for this sampling bias towards variable sites. Gap-filling used early/late season measurements from a different year at the same site, if available, and with a scaled early or late season measurement if not. Scaling factors were based on the observed mean seasonal variations from sites with both early and late summer data (0.35 for early to late season scaling in dry sites, or 1.4 for late to early season scaling of wet sites). This method allowed us to fill in missing data in 59 of the 90 sites, adding 91 data points to the original set of 347 subsite-aggregated measurements. Thirty-one gap-filled points used data from the same time of year but a different year, while 17 were in locations with no early summer measurements, and 43 in locations with no late summer measurements. We explored the effects of this gap-filling on model results, and verified that results were minimally sensitive to this approach, in terms of both modeled VWC values (prediction) and the relationships between modeled VWC and covariates (explanation). Although this analysis showed that missing data do not appear to be causing a significant bias in the results, the gap-filled dataset has been used throughout the modeling process to ensure that the data are balanced and complete.

2.7. Statistical models used

Two different statistical models were used to relate VWC to topographic, vegetation and fire history predictors: (i) a random forest model and (ii) a generalized linear mixed effects model. Both models predict continuously valued VWC using current vegetation type, vegetation type in 1970, upslope area, slope, aspect index, elevation, topographic position index (TPI), topographic wetness index (TWI), distance from nearest stream, year of measurement (2014, 2015, or 2016), day of year the measurement was taken (e.g. 152 for June 1), years since last fire, times burned since 1970, and maximum fire severity (unchanged, low, moderate, or high) as covariates. The current and 1970 vegetation types use the following categories: sparse meadow, dense meadow, shrub, aspen, and conifer.

Using two statistical approaches allowed us to capitalize on the relative advantages of each - primarily the ability of a random forest model to address nonlinearity in relationships between covariates and outcomes, and the relative ease of interpreting a linear regression model. The comparison between the two modeling approaches also provides a check on the consistency of interpretations made from the data.

2.7.1. Random forest model

Random forest models predict a continuous variable by creating a large number of regression trees, each based on a random subset of all possible covariates. The predicted values from all of the trees is then averaged (Breiman, 2001). Each regression tree divides the data into smaller and smaller groups, or nodes, until a stopping criterion is reached. The data in each parent node is divided into two child nodes based on one of the predictors, and the division that maximizes the separation in values between the two child nodes is selected at each step. The value of a new point in covariate space is computed by following the path from the first node to the appropriate terminal node. The random forest method can describe non-linear responses between variables and predictors, and avoids over-fitting that can result from using only one regression tree (Grömping, 2009; Kane et al., 2015; Prasad et al., 2006).

We used the RandomForest package in R (Liaw and Wiener, 2002) to fit a random forest model, and set the minimum node size to 5 and the number of trees to 500, the number that minimized the RMSE of the model. The impact of different covariates on modeled VWC was quantified using the *importance* and *partial dependence*. The *importance* of a covariate in a random forest model is calculated using the change in model error when a covariate is included or excluded as a covariate when training the model (Liaw and Wiener, 2002). The *partial dependence* describes the response of a dependent variable to individual covariates, while controlling for the effects of other covariates. For example, partial dependence could describe the influence of elevation on modelled VWC, independently of variation in other covariates. To assess the partial dependence, VWC would be computed for all possible values of the other covariates (vegetation cover, slope, aspect, time since fire, etc.) holding elevation constant. The resulting VWC values would be averaged. This procedure is repeated for different constant values of elevation to visualize the mean VWC response to changing elevation (Appendix D).

2.7.2. Linear mixed effects model

The VWC data were also fit with a generalized linear mixed effects model, referred to subsequently as "linear model" (Clark, 2007). This statistical modelling method is widely used, and can account for spatial autocorrelation between sub-sites. Spatial autocorrelation is often exhibited by large scale moisture patterns (Western et al., 1998).

The linear model was trained on the same data as the random forest model, using the lme function in R and assuming a spherical spatial correlation structure (Pinheiro et al., 2015). Vegetation cover was treated as a random effect (as in Chen et al., 2012; Omuto et al., 2010), allowing each vegetation type to have a separate intercept. We separated vegetation type by current and 1970 cover. All other covariates were treated as fixed effects, and were normalized to have values between 0 and 1 so that the magnitudes of model coefficients are comparable. For the categorical covariates of measurement year, fire severity, and times burned, we coded dummy variables, set to 0 or 1 for each data point by category (UCLA: Statistical Consulting Group, 2017). For example, two dummy variables were created for "year": the first was set to 1 if the measurement year was 2014 and 0 otherwise; the second variable was set to 1 if the measurement year was 2015 and 0 otherwise. Year 2016 was left as the intercept. The coefficients on these variables represent the relative change in VWC in 2014 or 2015 compared to 2016.

The final model takes the form

$$VWC(veg, x) = C_0(veg) + \sum_{i=1}^{n} C_i x_i$$

where VWC is the predicted water content, *veg* is the vegetation transition from 1970 to 2012, C_0 is an intercept unique to each vegetation category, x is a vector of n covariates, and C_i are model coefficients.

2.7.3. Model performance

Model performance was evaluated using a cross validation procedure in which all data measured within a random subset of X% of all sites were selected as training data, and used to predict VWC in the remaining 100-X% of sites. X varied from 70-90% of the data, and 100 iterations of the cross validation were performed for each value of X. This cross validation was designed to avoid spurious outcomes due to potential autocorrelation within sites (i.e. across subsites). Model performance was evaluated using root mean squared error (RMSE) and correlation coefficients. The mean and range of model performance across all 100 iterations provides an indication of the model skill in extrapolating beyond the observation points.

2.7.4. Simulations of soil moisture response to landscape change

Once the statistical models were trained to field measurements of VWC, the models were used to upscale soil moisture measurements to the whole ICB on a 10 m resolution grid, based on the maps of topographic covariates, fire history, and vegetation. These watershed-scale estimates were made using both contemporary and historical vegetation coverage and fire histories, providing insight into potential changes in soil moisture induced by the managed wildfire policy. To run the model to represent 1970 conditions, the "year" covariate was set to either 2014, 2015, or 2016 - effectively modeling VWC subject to the land cover and fire history from 1970, modulated by 2014–2016 climatic conditions.

3. Results

3.1. Field measurements

3.1.1. Relating surface and root-zone soil moisture

Both pre-dawn leaf water potentials and comparisons between near-surface and deeper subsurface soil moisture support the existence of a relationship between surface soil moisture and overall water availability at a measured site, although this relationship is not perfect. Predawn leaf water potentials were correlated with shallow soil moisture with a correlation coefficient of 0.69 (Fig. 3(A)). The greatest sensitivity of leaf water potential to VWC was observed for VWC below 0.08. A logarithmic function provided a good fit ($R^2 = 0.61$) to the observed relationship between leaf water potential and soil moisture. At the weather stations, the correlation coefficient between daily VWC at 12 cm and at 60 cm (during the summer months of May–August) was 0.98 for the closed canopy and shrub sites and 0.79 for the wet meadow site, and correlation between 12 cm and 90 cm–1 m soil moisture was 0.95 for closed canopy, 0.94 for shrub, and 0.77 for wet meadow (See Fig. C.1 for plots of soil moisture at all three depths). Combining data from all 3 stations, shallow soil moisture was strongly correlated to 60 cm soil moisture ($\rho = 0.96$) in the months of May-August, and well correlated to deep soil moisture ($\rho = 0.91$) (Fig. 3(B) and (C)). While surface soil moisture is not a one-to-one indicator of soil column water availability in the ICB, spatial variations in surface soil moisture appear to indicate spatial variation in water availability to plants and across the soil profile during the growing season.

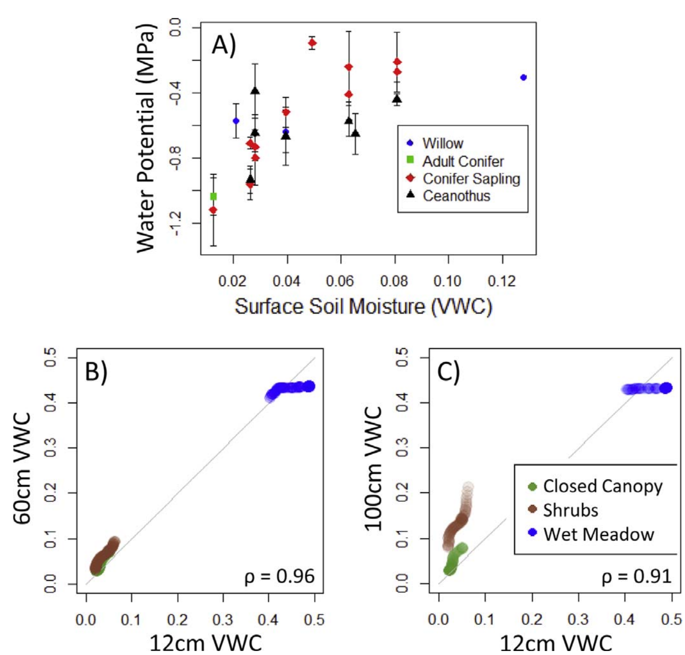

Fig. 3. Relationships between shallow and deep soil moisture. (A) A positive trend between surface soil VWC and water potential suggests that when surface soil moisture is low the root zone also has low moisture (and therefore a more negative water potential). Each point represents mean pre-dawn leaf water potential at a given location in conifers, willows, or ceanothus. Error bars give the standard deviation within each plant type at each site. (B-C) Continuous soil moisture measurements at three locations from May 20 to August 10, 2016 show shallow and deep daily measurements of VWC are closely related. Plot B shows measurements at 12 cm and 60 cm, with a correlation of 0.96, while C shows 100 cm vs. 12 cm, with a correlation of 0.91.

3.1.2. Observed relationships between VWC and vegetation type

Summer surface soil moisture content varied strongly across vegetation types, both in terms of mean or median VWC per vegetation type, and in terms of the variability associated with each vegetation class. To represent this within-class variability, data are presented as violin plots (Fig. 4). These plots show the distributions of data in different categories of pre-fire and contemporary vegetation. Persistent wetlands - areas that were mapped as dense meadow from the 1969/1970 aerial photographs and continued to be identified as such in all subsequent mappings using more recent aerial photos - had the highest moisture content of all sites. Conifer forests that burned and regenerated as dense meadows by 2012 were the next wettest vegetation category. Despite the drought conditions during the study, saturated soil was present in some of the dense meadows and persistent wetlands through to the late summer in every year. Soil moisture measurements were bimodal for burned dense meadows (all times) and persistent wetlands (late summer only), with most measurements either very wet or very dry (potentially due to small variations in elevation above a shallow water table).

In a mean sense, dense meadows were distinct from and much wetter than other vegetation categories, with mean VWC of 0.38 in May and 0.28 in August. At the beginning of the summer, persistent conifer sites had the next-highest mean VWC (0.11 across all conifer species), but dried rapidly and were comparable with other non-wetland vegetation types by August (0.06 VWC). There was a large range of variability within the conifer sites relative to other vegetation types. Conifer sites dominated by PICO had significantly higher mean VWC throughout the summer than other non-meadow vegetation (2.7 times higher under PICO, $p < .0001$ according to one-sided *t*-test). As discussed in Section 2.4, PICO sites were grouped with other conifers in the statistical model. We verified that this grouping did not result in changes in predicted VWC of more than 0.03, compared to statistical models representing PICO separately.

Shrublands and sparse meadows had comparable mean soil moisture values at the end of May (0.10 and 0.09, respectively), but the sparse meadows dried more rapidly, dropping to 0.04 mean VWC by June (data not shown) compared to 0.07 for shrubs (statistically different according to one-sided *t*-test, $p = .001$). The difference between June VWC values under these vegetation types is slightly lower and less significant when data is mean-aggregated by site rather than using each individual measurement (mean VWC = 0.05 for sparse meadow and 0.07 for shrubs, $p = .07$). In June, only 20% of VWC measurements in shrub sites fell below 0.03, whereas such low values were more common in sparse meadow or conifer sites (40% for both). By August, however, all vegetation types except for dense meadow and PICO had similar distributions of moisture.

3.2. Modeling results

3.2.1. Model performance

Cross validation results indicated that the random forest model provided an excellent fit to training data (mean Pearson's correlation coefficient, $\rho = 0.98$), and a robust, but weaker fit to test data (mean $\rho = 0.81$). Random forest model fits to all 2014–2016 soil moisture observations are shown in Fig. 5. The linear mixed effects model did not fit the training data as well ($\rho = 0.87$), and achieved comparable performance to the random forest model when predicting test data ($\rho = 0.79$). The results shown in Table 1 are representative of the full

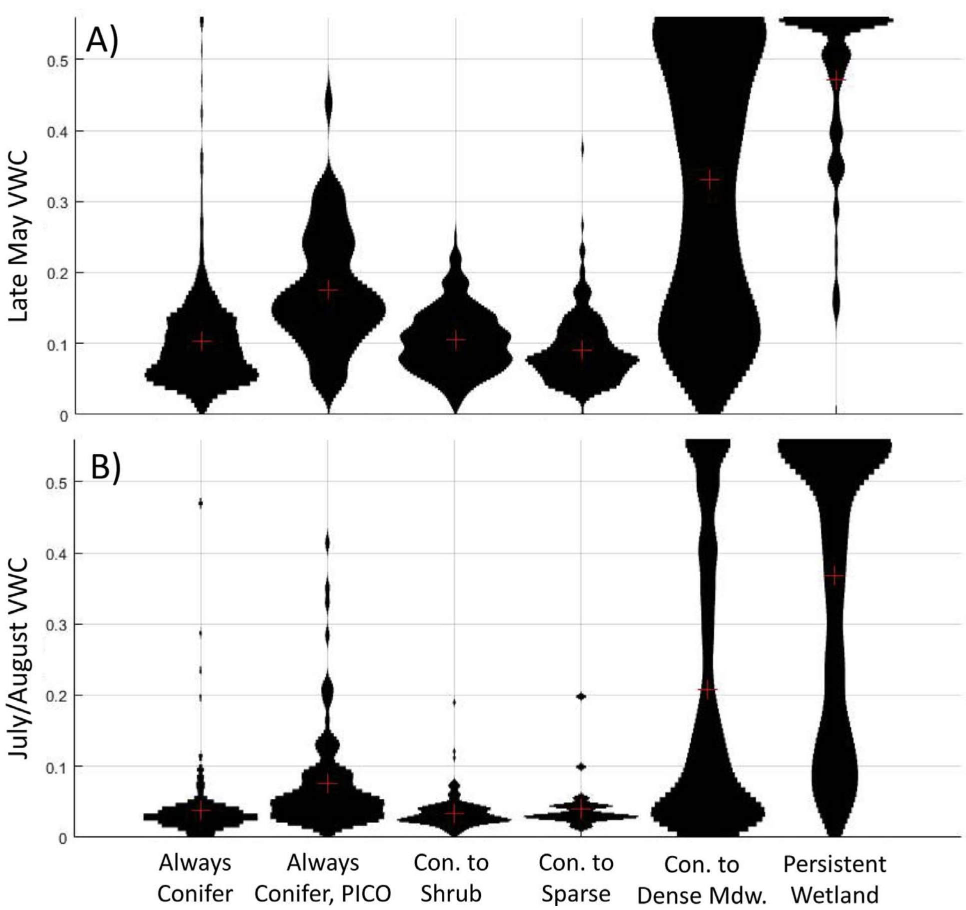

Fig. 4. Soil moisture measurements under different vegetation categories. Violin plots show the distribution of soil moisture measurements from all three summers, from either late May (A) or July–August (B). The first two vegetation categories are always conifer (conifer cover in both 1970 and 2012) and always conifer with PICO dominating currently. The next three categories, con. to shrub, con. to sparse, and con. to dense mdw., are sites where burned conifer forests were replaced by shrub, sparse meadow, or dense meadow. The final category, persistent wetland, includes sites that were dense meadow in both 1970 and 2012 (all such sites were wetlands). For simplicity, less common vegetation categories and June measurements are not shown. The width of the shape for each category is proportional to the number of observations at that VWC value, similar to a histogram. Red crosses show the mean within each vegetation category.

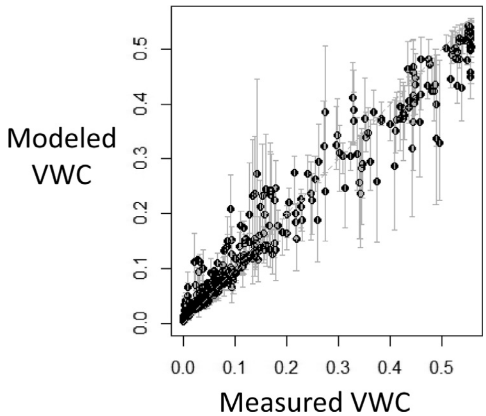

Fig. 5. Random forest model fit to observed soil moisture. All observed data from 2014–2016 is included. Error bars show the range of the 25th–75th quantiles of results from all trees within the random forest model.

Table 1
Mean and range of correlation coefficients (ρ) from 100 cross validation runs of two different models used to fit observed VWC data. Training data includes a random 80% of measurement sites, while test data includes the other 20%. Data is aggregated by subsite.

	ρ, Random Forest Mean (Min–Max)	ρ, Linear Model Mean (Min–Max)
Training Data	0.98 (0.98–0.98)	0.87 (0.84–0.90)
Test Data	0.81 (0.63–0.95)	0.79 (0.63–0.90)

suite of cross-validation exercises and show summary results for an 80:20 split between training and test data. They suggest that the random forest model may be overfitting the training data (Shmueli, 2010). Given the similarity in model performance, and to avoid duplication, model results presented here primarily use the random forest model output, which captures nonlinear relationships, and avoids some unrealistic VWC predictions (e.g. $VWC > 0.6$ or $VWC < 0$) made by the linear model. We refer to the linear model results to assist in interpretation of soil moisture sensitivity to covariates, and for checks on consistency between the models.

Numerous consistency checks verified that details of the training data organization (e.g. splitting versus lumping PICO with other coniferous forests, including or avoiding gapfilling to avoid early/late season bias in dry/wet sites) did not significantly impact model predictions, structure, or performance. For example, there was a correlation of 0.99 between VWC values from a model trained on observed data only and values from a model trained on gap-filled data. The mean difference in VWC between these two versions of the random forest model was 0.01, with a maximum difference of 0.06 at any subsite. Primarily, bias correction resulted in lower predictions of late summer soil moisture values, relative to the raw data, which we expect to be reasonable.

Table 2
Pearson's correlation coefficient of subsite-aggregated VWC compared to covariates (excluding categorical covariates such as vegetation).

Covariate	Correlation w/ VWC
TWI	0.52
Years Since Fire	0.19
Elevation	0.18
Upslope Area	0.17
Year	0.11
Aspect	0.09
Times Burned	−0.14
Severity (max)	−0.20
Day of Year	−0.20
TPI	−0.22
Slope	−0.39
Dist. from River	−0.40

3.2.2. Sensitivity of VWC to landscape parameters and fire history

As shown in Fig. 4, significant differences in soil moisture attributes arose between vegetation classes. Table 2 shows correlations between VWC and other landscape characteristics, and suggests that there were not overriding individual correlations between VWC and topography, fire history or time metrics. Upon controlling for covariates via statistical models, however, clear distinctions in the relative importance of the covariates' influence on VWC emerged.

The random forest importance metric shows that contemporary vegetation was the most important predictor of soil water content, and pre-fire vegetation was also in the top three most important (Fig. 6 and Table 3). TWI was one of the most important predictors of VWC in the random forest model, and had moderate predictive power in the linear model; slope had a strong influence on soil moisture in both models (see Table 3, Fig. 6, Table 4 and Fig. D.2). Both models agreed that years since fire and times burned did not have an important impact on VWC compared to other covariates.

The partial dependence metrics for the random forest model show that soil moisture is more likely to be high at sites with low slopes, low topographic position index, and near rivers or creeks - that is, in valley bottoms (Fig. 7(B), (D), and (F)). Soil moisture increased slightly with elevation and with aspect index (Fig. 7(A) and (C)). Topographic wetness index (Fig. 7(E)), slope (Fig. 7(B)), and upslope area produced threshold-like responses in VWC. Locations that were unburned or burned at low severity were more likely to have high VWC (Fig. 7(G)–(I)), although this relationship varied with vegetation type. For example, soil under conifer stands that regrew following high severity fire had the highest mean VWC of all conifer stands (data not shown).

The sign of the linear model coefficients for each covariate matched the sign of the slope of linear fits to the random forest partial dependencies, with the exception of times burned which had low significance in the linear model (Tables 4 and 3, Fig. 7). In the linear model, day of year had a greater coefficient than year (−11 vs. 3), confirming that within-year variability is more important than interannual variability. Again in agreement with the random forest results, topographic covariates generally had more influence on VWC than fire history according to the linear model (in terms of coefficient magnitudes as well as statistical significance).

3.3. Time dependence of soil moisture

The relationships in VWC between sites were consistent over all years, but some variation in individual sites did occur from year to year, and different years varied slightly in the mean. For most sites, 2014, which followed one of the lowest winter snowfalls on record across the Sierra Nevada, had the lowest soil moisture. This year to year variability had low importance in the random forest model, relative to the vegetation and topographic differences (Fig. 6 and Table 3). There were notable small differences, however: mean VWC was 0.01 higher in 2016 (the wettest year) compared to 2014 (the driest summer) on average, independent of all other covariates (Fig. 8(A)). This difference in means was statistically significant ($p < 1e-10$) according to a *t*-test performed on 100 cross-validation runs.

3.3.1. Summer moisture loss under different vegetation types

In contrast to the small year-to-year variability, within-year variation was relatively large (Fig. D.1). The rates of summer dry down could be estimated at 24 sites where soil moisture measurements were available at three dates (usually May, June, and late July or early August) by fitting a linear equation to the three data points. This linear fit gave a mean net loss of approximately 0.1–0.2 mm/day over the summer for all vegetation types except for permanently flooded

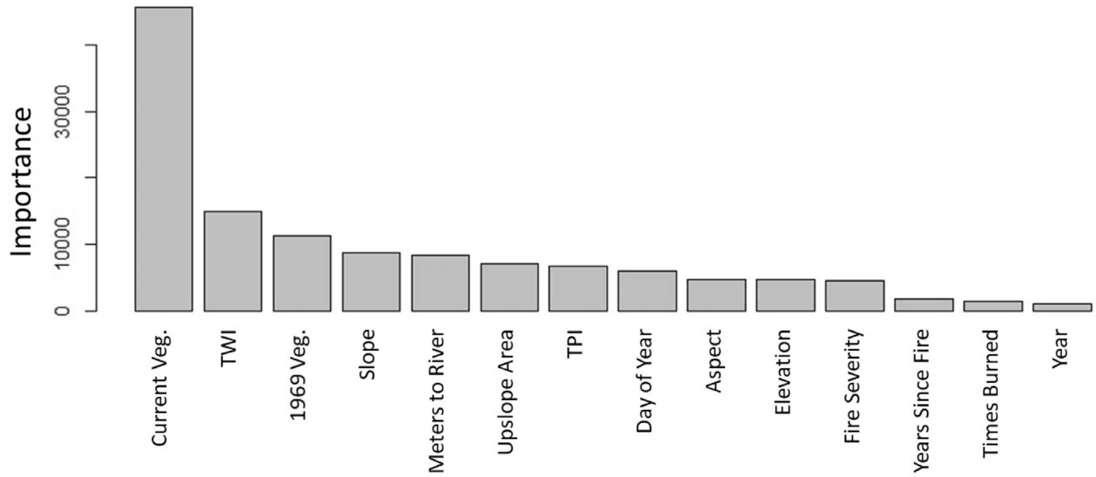

Fig. 6. The relative importance of each covariate to the random forest model. Importance is related to the reduction in model error when that covariate is included. The covariate with the highest importance is the current vegetation type. Topographic wetness index (TWI), vegetation type in 1970, slope, and distance from the nearest river (or creek) are the next most important covariates for predicting VWC. Years since fire, times burned, and the year of measurement all have a relatively small effect on the model predictions.

Table 3
Random forest model of soil moisture. Importance is given in terms of the mean and standard error of the percent increase in mean squared error when the covariate is removed. The final column gives the sign of the slope of linear fits to the partial plots for each numerical covariate (+ means that an increase in the covariate generally corresponds to an increase in VWC).

Covariate	Mean Importance (% change MSE)	Standard Error	Sign of Relationship
Current Veg.	211.9	4.4	N/A
TWI	53.6	2.9	+
1970 Veg.	36.9	2.3	N/A
Slope	32.7	1.7	–
Meters to River	31.9	1.8	–
TPI	25.6	1.4	–
Upslope Area	21.2	1.5	+
Fire Severity	17.5	1.1	–
Aspect	15.6	0.8	+
Elevation	15.4	1.0	+
Day of Year	13.2	0.6	–
Times Burned	4.8	0.6	–
Years Since Fire	3.7	0.6	+
Year	1.5	0.3	+

meadows (which did not dry). This results in a mean VWC drop of approximately 0.09–0.12 across the summer. The data were also normalized by dividing by the mean VWC at each site, in order to give the slope of the linear fit (the drying rate) as a percent per day. Using this normalizing method, forested hillslopes and sparse meadows dried at ≈ 2%/day, shrublands and riparian areas at ≈ 1%/day, and permanent wetlands did not dry out. Although these average values are useful for approximating seasonal water loss from shallow soils, the random forest model suggested that sharp decreases in soil moisture occurred at the end of May (corresponding to the end of snowmelt) and in late June (corresponding to peak temperatures), rather than drying proceeding uniformly throughout the summer (Fig. 8(B)). Similarly nonlinear drying trends were observed at the weather station TDR profiles (Fig. C.1).

3.3.2. Model simulations of soil moisture response to landscape change

Fig. 9(A) and (C) shows the results of upscaling the random forest model to the whole ICB. As shown, the resulting soil moisture predictions appear reasonable - no unrealistically high VWC values were predicted (Fig. 9(C)), and the spatial patterns appear realistically correlated and do not display isolated, erratic, high or low values, including in areas of the watershed where no observations were made. Fig. 9(B) and (D) shows an example of modeled difference in VWC

Table 4
Generalized linear mixed effects model of soil moisture. Random effect intercepts are different for each vegetation category (combining 1970 and 2012 vegetation). “Sparse” indicates sparse meadow and “Meadow” indicates dense meadow. Coefficients and their standard errors (SE), *t*-values, and *p*-values are shown for normalized continuous covariates as well as categorical covariates set to 0 or 1. Coefficients for categorical covariates represent a computed effect versus a given reference value. The *p*-values are the results of a marginal analysis of variance on the model.

Random effects:

Veg 1970	Conifer	Shrub	Conifer	Sparse	Sparse	Conifer	Aspen	Meadow	Conifer	Conifer	Meadow
Veg 2012	Sparse	Shrub	Conifer	Conifer	Sparse	Shrub	Aspen	Conifer	Aspen	Meadow	Meadow
Intercept	0.19	0.20	0.21	0.21	0.21	0.22	0.25	0.25	0.38	0.40	0.52

Fixed effects coefficients and significance:

Continuous Covariate	Coefficient	SE	*t*-val.	*p*-val.	Categorical Covariate	Coefficient	SE	*t*-val.	*p*-val.
Slope	−0.18	0.04	−4.2	0.0000	Year 2014 vs. 2016	−0.04	0.01	−2.7	0.0071
TPI	−0.17	0.06	−3.0	0.0032	Year 2015 vs. 2016	−0.04	0.01	−2.7	0.0067
DOY	−0.13	0.02	−7.4	0.0000	Mod. Severity vs. Low	−0.04	0.01	−3.1	0.0022
Meters to River	−0.01	0.06	−0.2	0.8045	High Severity vs. Low	−0.04	0.02	−2.4	0.0180
Time Since Fire	0.00	0.06	0.0	0.9647	Burned 1*X* vs. Unburned	0.04	0.07	0.8	0.4450
Aspect	0.01	0.02	0.7	0.4883	Burned > 1*X* vs. Unburned	0.02	0.05	0.4	0.7227
Elevation	0.02	0.03	0.7	0.4760					
Upslope Area	0.02	0.02	1.0	0.3210					
TWI	0.08	0.04	1.9	0.0650					

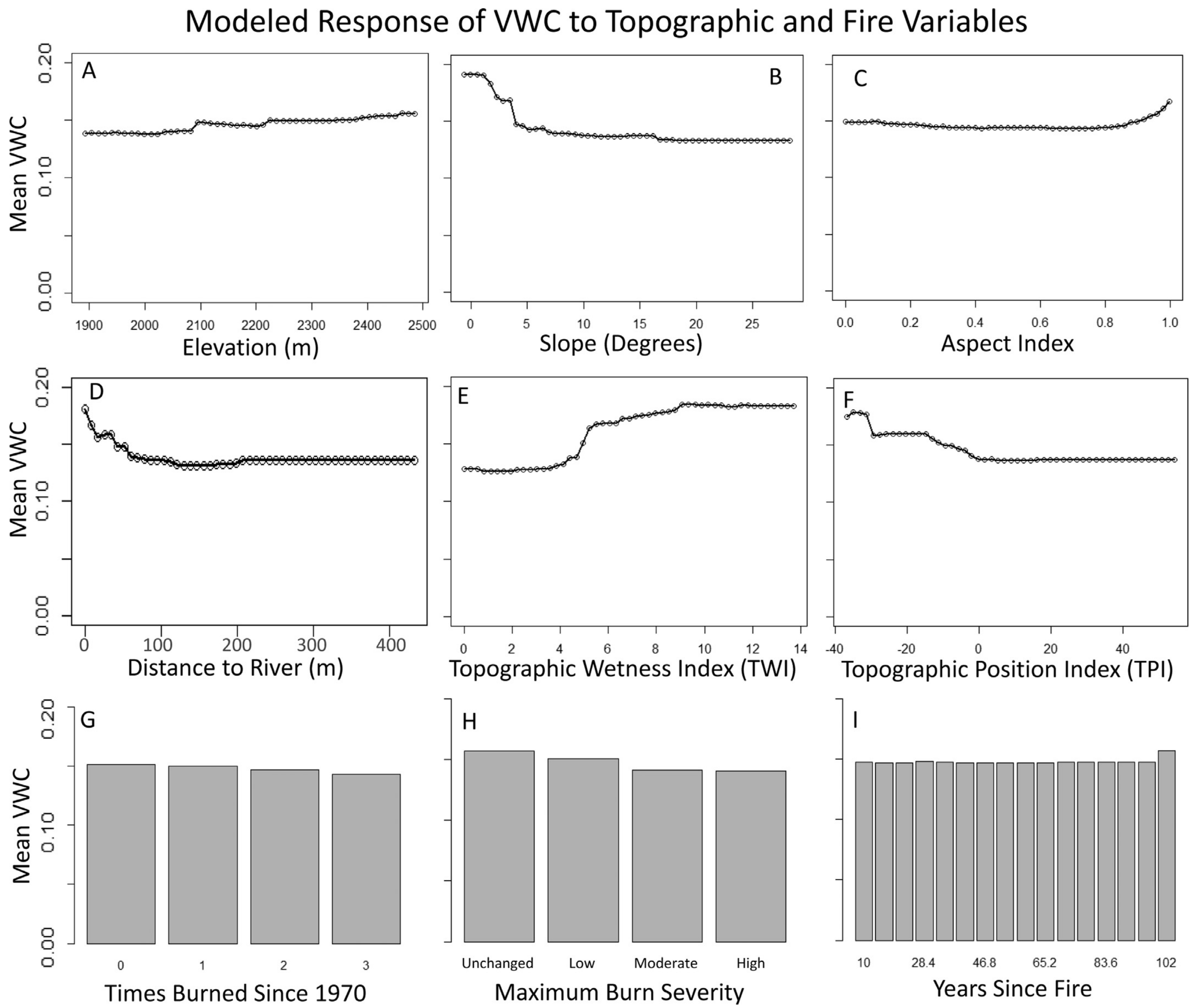

Fig. 7. Modeled changes in soil moisture across ranges of values for topographic and fire history covariates. Partial dependence of VWC on 9 covariates according to the random forest model are shown: elevation, slope, aspect index, distance to nearest river/creek, topographic wetness index (TWI), topographic position index (TPI), times burned since 1970, maximum severity, and years since fire.

between current conditions and fire-suppressed conditions. Specifically, this difference is calculated by modeling VWC with contemporary vegetation and fire history and then subtracting modeled VWC using 1970 conditions. Both the contemporary and 1970 models set the date to mid-August and set the "year" covariate to 2014 (effectively using 2014 climate). A positive value in Fig. 9(B) indicates that soil moisture is higher under 2014 conditions relative to 1970. At the basin scale, minimal differences in spatially averaged surface soil moisture are predicted between the fire suppressed and contemporary conditions (changes in mean basin-scale VWC < 0.02 for any model version). Dramatic changes, however, were predicted in the wetness of individual sites under all tested versions of the statistical models. Burned forest sites that regenerated with dense meadows (potentially wetland) vegetation increased in predicted summer VWC by as much as 0.31 (Figs. 10 and 9(D)). Variability in the VWC changes at these sites were associated with differences in TPI (larger increases in valley bottoms) and fire history (larger increases following low severity fire, relative to high severity fire, see Fig. 11). These large local increases in soil moisture, however, were offset by widespread, minor decreases in soil moisture; with the greatest decreases (down to -0.24) modeled in locations where conifers encroached on meadows. Using 2015 or 2016 as the contemporary year instead of 2014 resulted in only small differences in the map, and magnitude, of change.

The small magnitude of basin-scale change can be attributed to the relatively small changes in VWC estimated for the most common vegetation transitions. For example, from 1970 to present, 55% of the

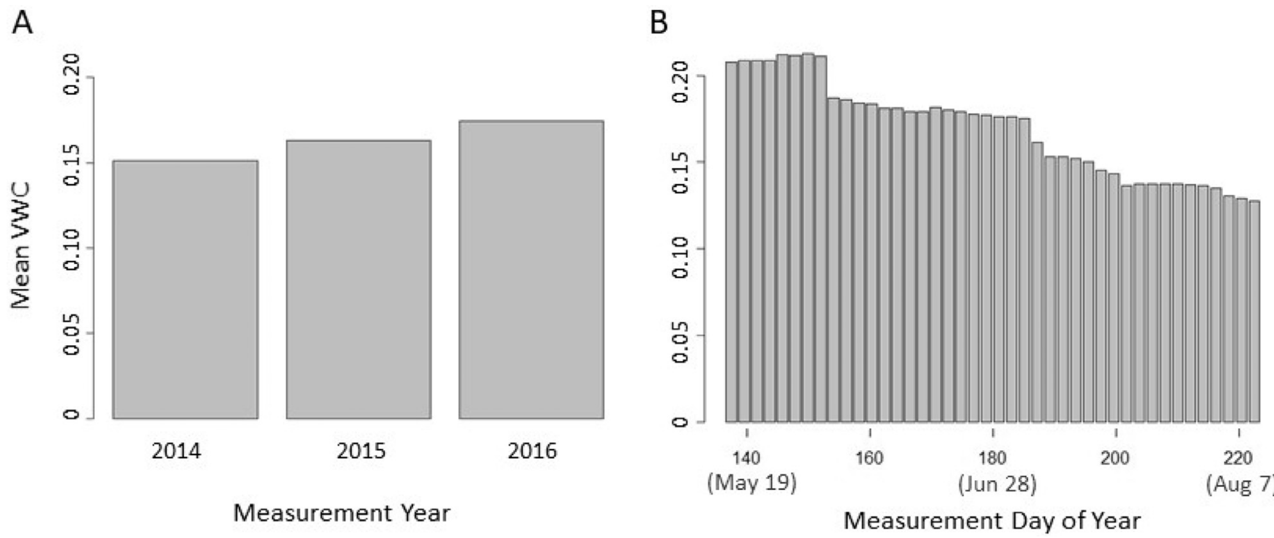

Fig. 8. Modeled changes in soil moisture over time. Partial dependence of VWC is shown for (A) the measurement year and (B) the number of days after the previous December 31 that the measurement was taken, according to the random forest model.

ICB's vegetated area was either permanently forested or burned and regrew as conifer forest (Table 5). Burning these areas did not result in large predicted changes in VWC: at most these sites increased in VWC by 0.02 or decreased by 0.05 (Table 5). The largest changes in VWC were associated with vegetation transitions that impacted less than 2% of the basin area (Table 5, Fig. 9(D)).

4. Discussion

This study set out to determine how the changing fire regime in the ICB may have impacted its hydrology, by addressing a suite of related questions about soil moisture - (i) was it a useful indicator of ecologically relevant water availability?, (ii) was vegetation a valuable proxy for soil moisture spatial variability? and (iii) how did topography and fire history influence soil moisture? The combination of field

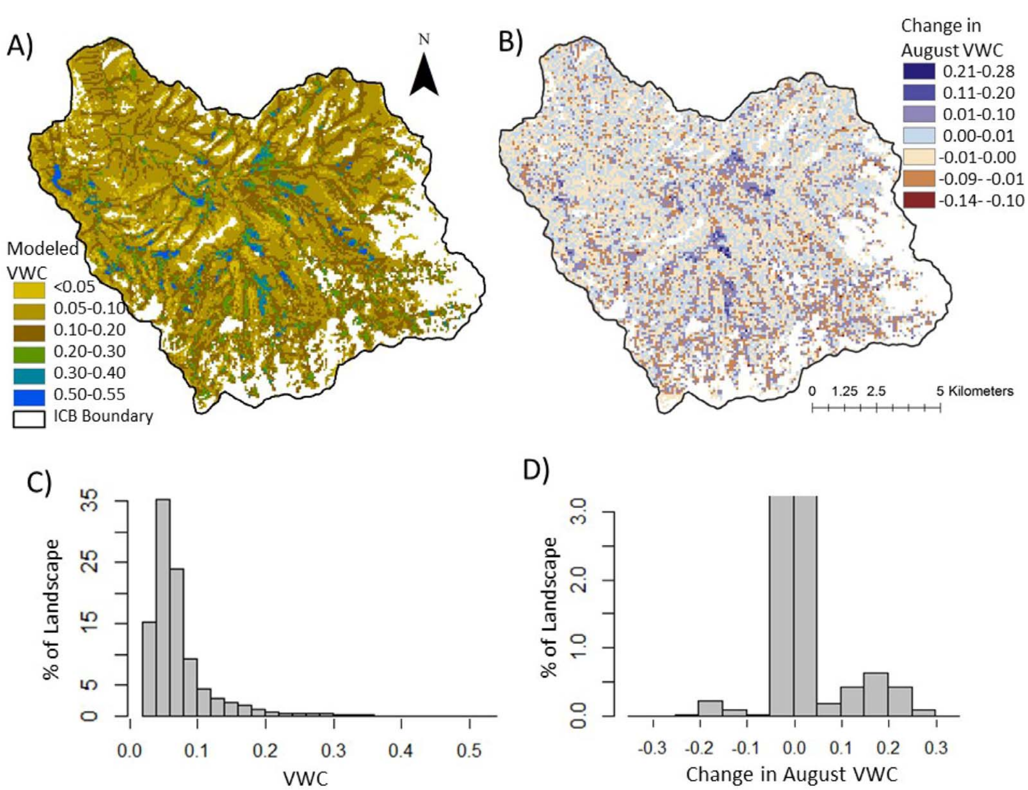

Fig. 9. Results of upscaling soil moisture using a random forest model. (A) Map of surface soil moisture given as volumetric water content (VWC) for June 9, 2014. Areas shown in white are exposed bedrock, talus, or lakes. (B) Change in VWC due to fire and land cover change, calculated as the difference between soil moisture under current conditions and what soil moisture would have been if there had been no fires in ICB since 1900. The measurement date covariate in the random forest model was set to early August 2014. Dark blue areas denote increases in soil moisture, while orange denotes a decrease and tan or pale blue indicates almost no change. (C) Histogram of modeled soil moisture across the ICB. (D) Histogram of soil moisture changes shown in (B); most VWC changes were less than 0.05 in magnitude (nearly 98% of the landscape), so the heights of these bars are truncated to better show the larger changes.

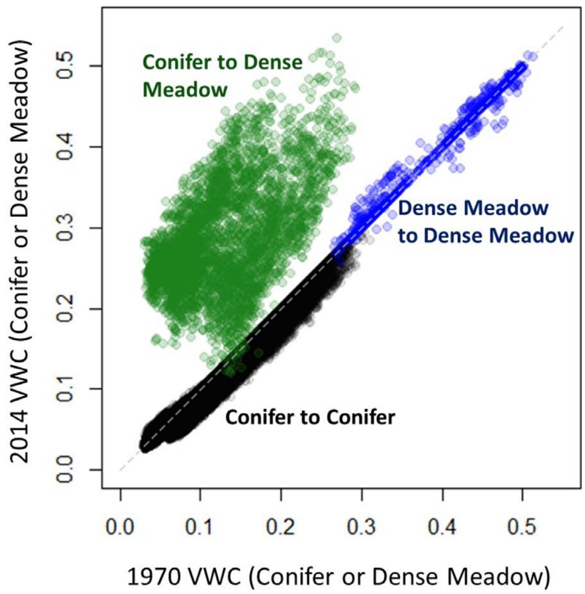

Fig. 10. Scatterplots of modeled surface soil moisture for June of 1970 to June of 2014. Only three vegetation transition types are included here: those that were conifer-dominated in both 1970 and 2014 (conifer to conifer, in black), dense meadow in both years (dense meadow to dense meadow, in blue), and those that were conifer-dominated in 1970 and transitioned to dense meadow by 2014 (conifer to dense meadow, in green).

measurements and statistical modeling at ICB provides insights into all these topics.

The study period of 2014–2016 coincided with a period of extended and severe drought in California characterized by both low precipitation and high temperatures (Dettinger and Anderson, 2015; Griffin and Anchukaitis, 2014). Although the summer of 2016 followed a winter of near-average precipitation, the Sierra Nevada was still considered to be in extreme to exceptional drought (http://www.droughtmonitor.unl.edu). Our results might be different if we were using measurements from a non-drought summer. Understanding hydrologic dynamics during drought conditions, however, is disproportionately important since small changes in water availability can have a very large impact during times of water limitation.

Table 5
Vegetation type transitions. Percent of total area experiencing each of the 9 most common transition types (all other types cover < 1% of the total watershed area), with the associated minimum, maximum, and median changes in mid-June VWC between 1970 and 2014 (Δ VWC), according to the random forest model (a positive number indicates an increase in soil moisture from 1970 to 2014 for an individual grid point).

1970 Veg.	2012 Veg.	Area (%)	Δ VWC Min.	Δ VWC Max.	Δ VWC Median
Conifer	Conifer	54.7	−0.05	0.02	0.00
Conifer	Sparse	17.3	−0.06	0.02	0.00
Conifer	Shrub	8.3	−0.06	0.02	0.00
Sparse	Sparse	4.3	−0.04	0.02	0.00
Shrub	Shrub	4.0	−0.04	0.02	0.00
Shrub	Conifer	3.5	−0.04	0.02	0.00
Sparse	Conifer	2.7	−0.05	0.02	0.00
Shrub	Sparse	1.9	−0.04	0.02	0.00
Conifer	Dense Meadow	1.6	−0.03	0.31	0.17

4.1. Is surface soil moisture a useful indicator of ecologically relevant water availability?

Both leaf water potential and continuous soil moisture measurements suggest that surface soil moisture provides a proxy for plant available water (or soil-profile water storage) in the ICB (Fig. 3). The relationship between shallow soil moisture and leaf water potentials in plants was variable, presumably due to variations in plant morphology, subsurface heterogeneity, and potentially variable rates of night-time transpiration which inhibit equilibration between leaf and root zone water potentials (Dawson et al., 2007; Sellin, 1999). Despite very dry soil conditions measured at some sites, plant water potentials remained relatively high. This may be related to the availability of non-soil water reservoirs. For instance, conifers in the Sierra Nevada may obtain as much as a third of their water from fractured rock beneath the developed soil (Bales et al., 2011; Royce and Barbour, 2001). Nonetheless, our small number of measurements from large, deep-rooted conifers had the lowest measured leaf water potential in areas with the driest measured surface soil moisture (Figs. 3(A) and B.1).

Strong correlations between surface and deep continuous soil moisture measurements support the value of shallow soil moisture as a proxy for site water availability (Fig. 3(B) and (C)), though these correlations vary with time, depth, and vegetation cover type. Despite the close relationship between shallow and deeper soil moisture, the relationship was non-stationary over the summer, and the non-

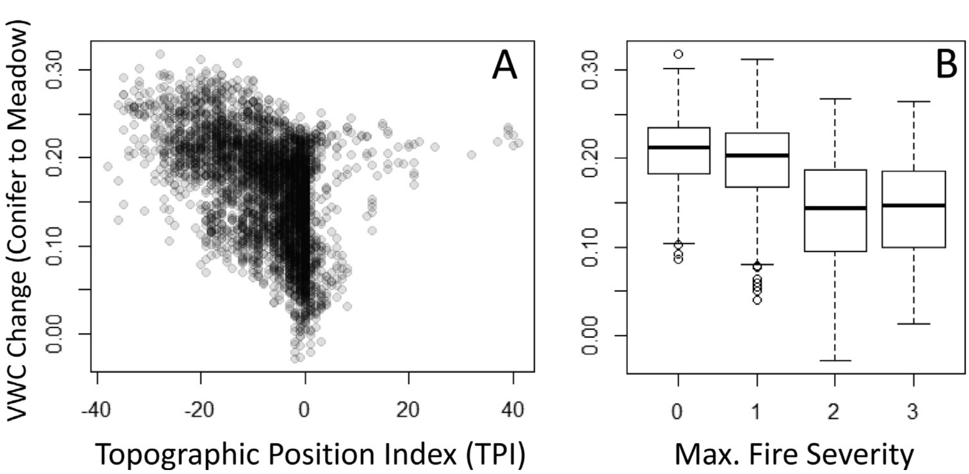

Fig. 11. Modeled increase in June VWC between 1970 and 2014 in areas that transitioned from conifer to dense meadow during this period. (A) TPI has a correlation of −0.47 with the change in VWC, and (B) fire severity (ranging from 0 = no change within a year of fire to 3 = high severity) has a correlation of −0.42. Results using late summer VWC were nearly identical.

stationarity varied with vegetation conditions. Soils at the instrumented wetland site (which had been forested prior to 2004) remained saturated at depth all summer, while in the forested site summer soil moisture was fairly constant with depth, and in the shrubland deeper soils contained twice as much water as shallow soil in the early summer of 2016 (Fig. C.1). These data raise the intriguing prospect that vegetation conversions from forest to shrubland or meadows could increase deep soil moisture stores significantly, despite only minor changes being observed in surface soil moisture - a prospect consistent with the shallower rooting depth of shrubs/grasses relative to mature trees. Using the weather station data to extrapolate soil moisture changes in the top meter of soil, we estimated a 7% increase in mean watershed soil moisture in early summer of 2014 relative to 1970 - compared to an estimated 2% drop in shallow soil moisture alone (Appendix E). This extrapolation has high uncertainty given the limited number of deep VWC measurements, but illuminates a possibility that deeper soil moisture stores are increasing due to fire regime shifts even in some places where surface soil moisture is not strongly affected. The general trends of our results would not change, however, with those areas that transition from conifer to dense meadow still experiencing the greatest increases in moisture (Appendix E).

4.2. Model performance

The linear and random forest models gave similar results in terms of covariates' influence on VWC as well as the predicted upscaled spatial pattern of soil moisture. The model predictions were also stable to the tested variations of model structure or input data treatment. Using cross validation, we found model correlation to test data of approximately 0.81 using random forest and 0.79 using the linear model. This was stable across different cross validation exercises undertaken. These model fits are strong in comparison to similar statistical models used to predict soil moisture in other studies (e.g. Western et al., 1999, found model predictions to have $\rho \leq 0.78$ for VWC on individual days, whereas our model has higher ρ and spans a range of dates) and are comparable to the performance of remotely sensed soil moisture products (e.g. Chan et al., 2016, found a mean correlation of 0.78 between time series of satellite-derived soil moisture and measured data).

4.3. Is vegetation a viable proxy for soil moisture?

Vegetation was the strongest predictor of soil moisture status within the ICB, eclipsing topographic factors (the next most important predictors) and fire history, which are discussed below. The importance of vegetation was strongly driven by the large differences in wetness between wetlands and other vegetation types (Fig. 4).

As discussed in the introduction, we anticipated this strong relationship between moisture and vegetation because multiple feedbacks influence their interactions. Vegetation changes can alter soil moisture through changes to water and energy balances, while soil moisture levels partially determine the type of vegetation which will establish following a disturbance. While the causal links between moisture and vegetation cannot be determined via this data analysis, the association of different vegetation types and transitions with different soil moisture states holds across the ICB, providing an avenue for using vegetation change as a proxy - albeit an imperfect proxy - for hydrologic change.

4.4. How did topography and fire history influence soil moisture?

Topography, and particularly the topographic wetness index, was an important determinant of wetness within vegetation types. Valley bottoms and other topographically convergent locations, as well as higher elevations, were associated with higher soil moisture. Surprisingly, south facing slopes had higher soil moisture than north facing slopes once other factors were controlled for, however this effect was not strong.

Model results suggested that, amongst conifer forests, soil moisture was elevated in both unburned areas and high severity burn areas, and lower in areas with low-moderate severity fire. Elevated moisture following high severity fire can be explained by reduced evaporating leaf area and plant water demand. High moisture in unburned sites could be due to reduced soil evaporation under unburned canopies, or it is possible that contemporary unburned sites failed to burn in the first place because of their relatively wet conditions. Amongst the remaining vegetation classes, soil moisture was generally lower in sites with frequent or severe fire histories. Interpreting the causal influence of fire on water availability is complicated in the ICB, because moisture availability and topography also determine where fires occur in this basin (Kane et al., 2015). Thus low soil moisture in frequently or severely burned sites (Fig. 7(G) and (H)) could reflect the effect of vegetation change on soil moisture status, or it could reflect the propensity for dry sites to burn more frequently.

The potential for dry sites to promote burning may also have caused the statistical model to overestimate soil moisture in the unburned 1970 scenario: (1) dry, fire-prone coniferous sites may be very rare within the basin today (and thus were not captured in the observations we made) after 40 years of managed wildfire, (2) unburned or low fire severity conifer sites may have escaped high severity fire due to pre-existing wet conditions. Overall, these issues may have biased the estimates of hydrologic change in the basin towards drying.

4.5. Influences of a changing fire regime on basin hydrology

Overall, the changing fire regime in the ICB appears to have impacted the hydrology of the basin, but in a highly spatially variable fashion (Fig. 9).

Large increases in water availability were associated with the $< 2\%$ of the basin area where burned forests regenerated as meadows. Other vegetation transitions, which occupy a larger proportion of the basin, resulted in minor changes in soil moisture, the sign of which varied with local topography and fire history (Table 5). Since fire-regime induced forest loss occurred over some 20% of the basin (Boisramé et al., 2017b), the constrained nature of the wet-up is suggestive of the confluence of other topographic, fire history or unobserved factors that govern the nature of these vegetation transitions and hydrologic changes.

There was large variability in soil moisture within vegetation transitions. For example, some areas where conifer transitioned to dense meadow following fire saw no change in soil moisture, while others saw VWC increases up to 0.31 (Fig. 10). This variability was largely driven by topography: flat landscapes (TPI near zero) were sometimes associated with decreased VWC in new dense meadows (Fig. 11) and also experienced the greatest drying from 1970 to the present day under other vegetation transitions (not shown). The largest modeled increases in VWC occurred in post-fire meadows that formed in topographically convergent areas. Convergent sites, however, did not always transition to dense meadows following stand replacing fires, showing that topography is not a perfect predictor of moisture increases.

The wet meadow areas sampled were variable in their water sources - some appear to be strongly snowpack dependent (revealed by wetter conditions in the near-average snow year of 2016 compared to extremely low snowpack in 2015), and some appear to be more dependent on summer rainfall (drier conditions in 2016 than 2015, mirroring trends in summer rainfall between the years). This could be due to variations in water sources, ranging from observable sources such as streams to unobservable sources such as springs or seeps (Ratliff, 1985). The diversity of hydrological drivers and responses associated with the sampled meadows is suggestive of a complex suite of processes linking vegetation, soil moisture, topography, and climate (Lowry et al., 2011; Rodriguez-Iturbe et al., 2007), all of which can interact with, shape, and be shaped by shifts in vegetation due to changing fire regimes (Neary et al., 2005). A deeper understanding of subsurface flow processes in ICB would allow us to better estimate past soil moisture distributions, but at present we are restricted to statistical relationships between soil moisture and surface topography, which cannot capture the effects of flows from springs.

Although conifer to dense meadow transitions and the associated increases in water availability are only associated with a small area in the ICB, these increases in water availability could nonetheless provide important hydrologic refugia for water-dependent plants or animals (McLaughlin et al., 2017). Wetlands also sustain summer baseflow in small streams, and thus have an impact on downstream ecosystems.

These transitions from relatively dry forests to wetter meadows may be an example of alternative stable states (Ridolfi et al., 2006). In areas that are prone to high soil water storage (due to topography and/or subsurface flow paths) forests can provide stabilizing feedback if the trees' high levels of transpiration maintain groundwater levels low enough for more trees to establish. On the other hand, wet meadows can remain stable via multiple mechanisms that maintain high water tables which then limit tree establishment (Fletcher et al., 2014; Ridolfi et al., 2006). A dry period can switch the system from the meadow stable state to the forested stable state by initiating a period of conifer encroachment (Helms, 1987), while fire or some other cause of tree mortality can return a forest to a stable meadow state (Fletcher et al., 2014). In either case, the vegetation transition is accompanied by a self-reinforcing transition in water storage. It is also possible that some of these meadows represent unstable states: if water levels are low enough that conifer establishment is not strongly drought-dependent, frequent disturbances such as fire may be necessary to prevent transitions back to forest (Helms, 1987). Either way, observed land cover changes (Boisramé et al., 2017b) and the moisture changes modeled here suggest that a frequent fire regime is necessary for the long-term maintenance of at least some of the wet meadows in the ICB, and thus the maintenance of associated high subsurface water storage.

4.6. Future work

Ongoing observations at the weather stations described here aim to explore how changes in vegetation canopy impact microclimatic conditions and local scale water balance, as an initial exploration of how vegetation changes may translate into changes in hydrologic drivers.

It is possible that water stores in deeper soils, or in the unmonitored fractured bedrock have increased due to the change in fire regime. Future work using hydrologic modeling will explore these possibilities.

5. Conclusion

Statistical models of the ICB indicate that vegetation can provide a useful proxy for soil moisture availability, and thus potentially its changes over time, provided that topographic and fire history effects can be controlled for. Vegetation was the most important predictor of variations in surface soil moisture; and surface soil moisture was related to both plant available water, and to measures of water availability in the surface 1m of soils. Thus, topographic and vegetation spatial information provided a scaling approach to link site based observations to basin-wide soil moisture regimes. Such an approach is widely applicable to watersheds with variable vegetation cover observable using remote sensing.

The model results did not indicate large changes in basin-averaged surface soil moisture in the ICB following restoration of the fire regime. Individual locations exhibited large increases in soil moisture following fire-induced vegetation conversions, while much of the remainder of the basin showed no change or weak drying trends. The basin scale estimates may be biased towards under-estimating the hydrologic impacts of these managed wildfire regime, however, due to a likely bias towards observing relatively wet contemporary coniferous forests, and possibly greater differences in deep soil moisture stores than shallow between vegetation types. Process hydrologic modeling is being used to further investigate these changes.

The most dramatic fire-related VWC increases shown by statistical models were associated with locations that were forested in 1970, experienced high severity fire, and were colonized by dense meadow. According to the model, most of these areas had elevated soil moisture compared to other forested areas even before burning, and became even wetter following the vegetation shift (Fig. 10). Based on this result and observations in the field, we believe that areas that transition from forest to dense meadow (rather than to a more xeric vegetation type) following fire have local topography and geology which facilitates high soil moisture storage in these areas. Such areas may even have been wetlands in the past, but in relatively dry years during fire suppressed periods trees were able to colonize (Helms, 1987; Norman and Taylor, 2005) and the high water demand of these trees further reduced the soil moisture. Once these trees and their high transpiration demand were removed, enough water was available for the soil to come closer to saturation, making the ground less favorable to tree seedling growth and more favorable for grasses and forbs.

Managed wildfire has wrought large changes in vegetation cover and structure in the ICB, and these have numerous documented benefits to resilience and ecological health (Boisramé et al., 2017a; Collins and Stephens, 2007; Ponisio et al., 2016). While we do not find evidence of large hydrologic responses to these changes, the hydrologic shifts that have occurred are likely to be broadly positive, creating ecologically and hydrologically valuable wet summer habitat. Given the uncertainties associated with the statistical modeling approach taken here, further efforts to apply process models to, and ultimately improve hydrological monitoring of, basins experiencing vegetation change through managed wildfire regimes should remain a research priority for watershed management.

Acknowledgments

Thank you to Yosemite National Park for permitting us to conduct research in wilderness areas.

Special thanks to Kate Wilkin and Brandon Collins for their field expertise, and to all of this project's field crew members and volunteers: Miguel Naranjo, Andy Wong, Perth Silvers, Jeremy Balch, Seth Bergeson, Amanda Atkinson, Tom Bruton, Diane Taylor, Madeleine Jensen, Isabel Schroeter, Katy Abbott, Bryce King, Zubair Dar, Katherine Eve, Sally McConchie, Lena Nitsan, and Chris Phillips (in order of appearance).

The vegetation maps were created by the authors as well as GIS technicians Julia Cavalli, Miguel Naranjo, and Melissa Ferriter, with guidance from Professor Maggi Kelly.

Funding: This work was supported by the U.S. Joint Fire Science Program (grant number 14-1-06-22); the National Science Foundation

EAR (grant number 1013339); Sigma Xi Grants in Aid of Research; the UC Berkeley SMART program; the Hellman Fellows Program; the UC Agriculture and Natural Resources competitive grant program; and the UC Berkeley Philomathia Graduate Fellowship in Environmental Sciences.

This project also used software resources provided by the UC Berkeley Geospatial Innovation Facility (gif.berkeley.edu).

Appendix A. Properties of sampling locations

Our sampling strategy attempted to cover the widest range of geographic variables possible within the ICB. This attempt was limited by safety and accessibility of many areas of the watershed. Although we did not sample the steepest parts of the ICB - as they are prohibitively difficult to access for measurements - the steepest areas are mainly rock, therefore they have few fires and do not store much soil moisture, making them less relevant to our study. Although our measurement sites do not always cover the full range of variability in physical characteristics, the measured span does include the median watershed value for every covariate (Table A.1).

Table A.1
The range of physical covariates for the watershed, labeled “All”, and for the soil moisture measurement locations, labeled “Measured”. The watershed (“All”) covariates are only calculated for the area between 1890 m and 2490 m in elevation, since this is the elevation range in which all known fires have burned in ICB. These covariates include slope (degrees), aspect (degrees from North, -1 indicates a horizontal surface), elevation (m), distance from nearest stream (m), Topographic Position Index (TPI), Topographic Wetness Index (TWI), upslope area (m^2 upslope of measurement), times burned in the record (going back to approximately 1930), Years since most recent fire (if no fire on record, marked as 101), Relative Difference Normalized Burn Ratio (RdNBR), and fire severity as a number from 0 = unburned to 4 = high severity.

Covariate	Min	Max	Mean	Median
Slope (Degrees) All	0	79	13	12
Slope (Degrees) Measured	0	31	8	7
Aspect (Degrees) All	−1	360	190	215
Aspect (Degrees) Measured	−1	360	184	217
Elevation (m) All	1890	2490	2270	2291
Elevation (m) Measured	1893	2487	2203	2192
Dist from River (m) All	0	681	128	102
Dist from River (m) Measured	0	436	83	67
TPI All	−63	201	−1	−2
TPI Measured	−38	55	−6	−7
TWI All	0	17	3	3
TWI Measured	0	15	4	4
Upslope Area (m^2) All	0	374,126	344	6
Upslope Area (m^2) Measured	0	51,417	1081	21
Times Burned All	0	5	1	1
Times Burned Measured	0	4	2	2
Years Since Fire All	5	101	32	14
Years Since Fire Measured	10	101	19	13
RdNBR All	0	3857	253	172
RdNBR Measured	0	1129	390	339
Severity All	0	4	2	2
Severity Measured	0	4	3	3

Appendix B. Leaf water potential measurements

This appendix presents details of the leaf water potential measurements used to relate surface VWC to root-zone soil saturation.

Fig. B.1 shows a stronger relationship between water potential (measured in PSI) and surface soil water content in the pre-dawn measurements compared to those in the afternoon. Certain species separate well in the afternoon measurements: *P. jeffreyi* has relatively low afternoon leaf water potentials, indicating that they are not losing much water to transpiration. The *Salix* species, on the other hand, all have high afternoon leaf water potentials, suggesting high levels of transpiration.

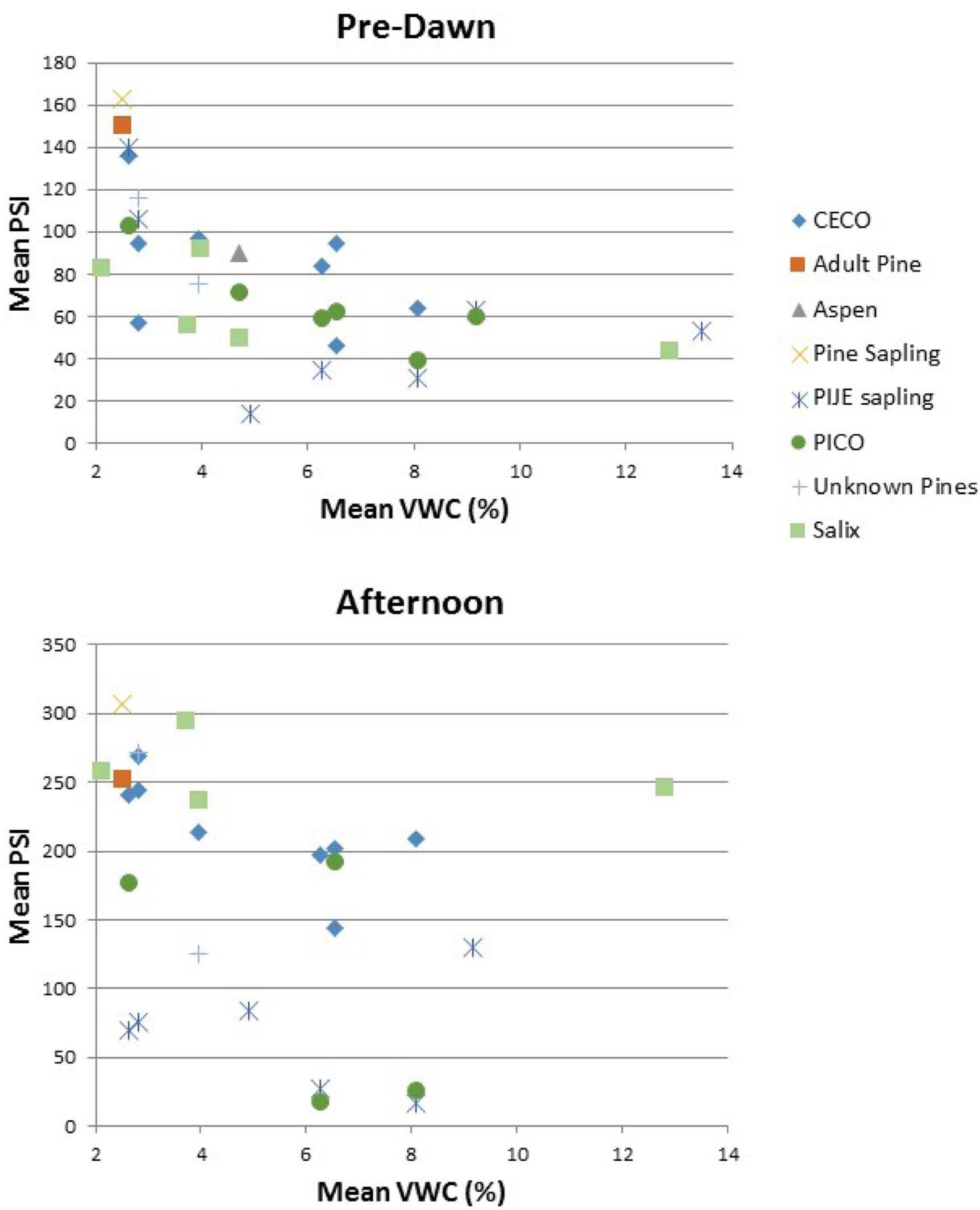

Fig. B.1. Leaf water potentials measured just before dawn and during mid-day, plotted agains surface soil water content (VWC). Each point on the plot represents the average of measurements in a given species taken at the same time of the same day, in the same location. The species are whitethorn ceanothus (CECO, *Ceanothus cordulatus*), aspen (*Populus tremuloides*), Jeffrey pine (PIJE, *Pinus jeffreyi*), lodgepole pine (PICO, *Pinus contorta*, willow (*Salix*), and unidentified pines (PICO or PIJE).

Appendix C. Continuous measurements

Three temporary weather stations installed in July 2015 monitor temperature, relative humidity, soil moisture, soil temperature, wind speed, and solar radiation in the ICB. Measurements are recorded every 10 minutes using a Campbell Scientific CR1000 datalogger (http://www.campbellsci.com).

All three stations are within an area that has burned twice, most recently in 2004. One station is in a low severity burn area with an intact, mature, mixed conifer canopy. The other two stations are in nearby burned areas with no mature trees within at least 25m. One of these non-forested stations is dominated by shrubs, and the other is in a wet, dense meadow dominated by grasses.

These stations are located within 200 m of each other in the southwest region of Illilouette Creek Basin, at an elevation of approximately 2100 m (close to the mean elevation of the forested area within the ICB, which is 2270 m). They are located uphill of the nearest trails and are over 3km from the nearest road, and therefore should not be affected by human infrastructure.

Time-domain reflectomer (TDR) probes were installed at three depths ranging from 12 cm to 100 cm at each weather station in order to capture subsurface water storage dynamics (Fig. C.1). Soil from three depths within each of the pits dug for these installations was analyzed by the UC Davis Analytical Laboratory for soil texture and percent organic matter (anlab.ucdavis.edu). The surface (top 10 cm) wet meadow soil sample was 13% organic matter. All other soil samples consisted of over 87% sand particles and less than 5% organic matter, even the deeper wet meadow soils, classifying them as loamy sand.

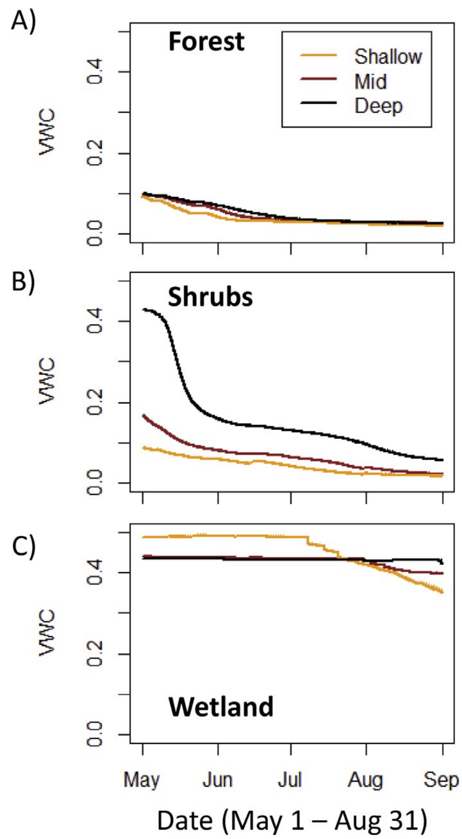

Fig. C.1. Soil moisture over the summer of 2016 measured at three weather stations with different dominant vegetation cover: dense conifer forest (A), shrubs (B), and wetland (C). The measurements are taken at depths of 12 cm (orange), 50–60 cm (brown), and 90–100 cm (black). (For interpretation of the references to color in this figure legend, the reader is referred to the web version of this article.)

Appendix D. Model details

We tested all covariates for collinearity, and found no correlations with absolute value above 0.7, which is a common cutoff to determine if collinearity will impact a model's ability to determine the impact of individual predictors (Dormann et al., 2013; Shmueli, 2010). We also tested the collinearity of all gridded data used in the model, not just locations where we measured, and the only high collinearity was between times burned and time since fire (correlation coefficient of −0.83, Table D.1). Even TWI and slope, which we would expect to be closely related, only had a

Table D.1
Table of Pearson's correlation coefficient (ρ) between pairs of covariates used in the random forest model for all measured locations and across all of the ICB. All covariate pairs with ρ > 0.4 are shown, out of 66 possible pairs.

Covariate 1	Covariate 2	ρ, Measured Sites	ρ, All ICB
TWI	Upslope Area	0.47	0.35
Time Since Fire	Times Burned	−0.45	−0.83
Elevation	RdNBR	−0.43	−0.44
Times Burned	RdNBR	0.06	0.43
Time Since Fire	RdNBR	−0.26	−0.53
Distance from Rivers	TPI	0.37	0.59
Elevation	Times Burned	−0.09	−0.52
Elevation	Time Since Fire	0.23	0.56

correlation coefficient of −0.25, and upslope area and TWI had a correlation coefficient of 0.47. Because of these fairly low correlation coefficients we determined that each of these three covariates provided different information to the model, and chose to include them all as predictors. There were three pairs of numerical (non-categorical) covariates used in the random forest model with correlation above 0.4 in absolute value (Table D.1).

Looking at all gridded data used in the model, not just locations where we measured, the pairwise correlations were not always the same as for our measured locations (Table D.1). We also found relatively high correlations (> 0.4) between geographic location (given by latitude and longitude) and elevation as well as times burned. For this reason (as well as low statistical significance in initial regression analysis), latitude and longitude were not included in the model, but this information still shows that there are spatial relationships that govern different covariates. There were also correlations between 1970 vegetation and time since fire due to wetland vegetation rarely burning, but this is not included in Table D.1 as vegetation is categorical rather than a numerical covariate.

Soil moisture changes throughout summer can be highly nonlinear, and the changes over summer can be very different in different locations

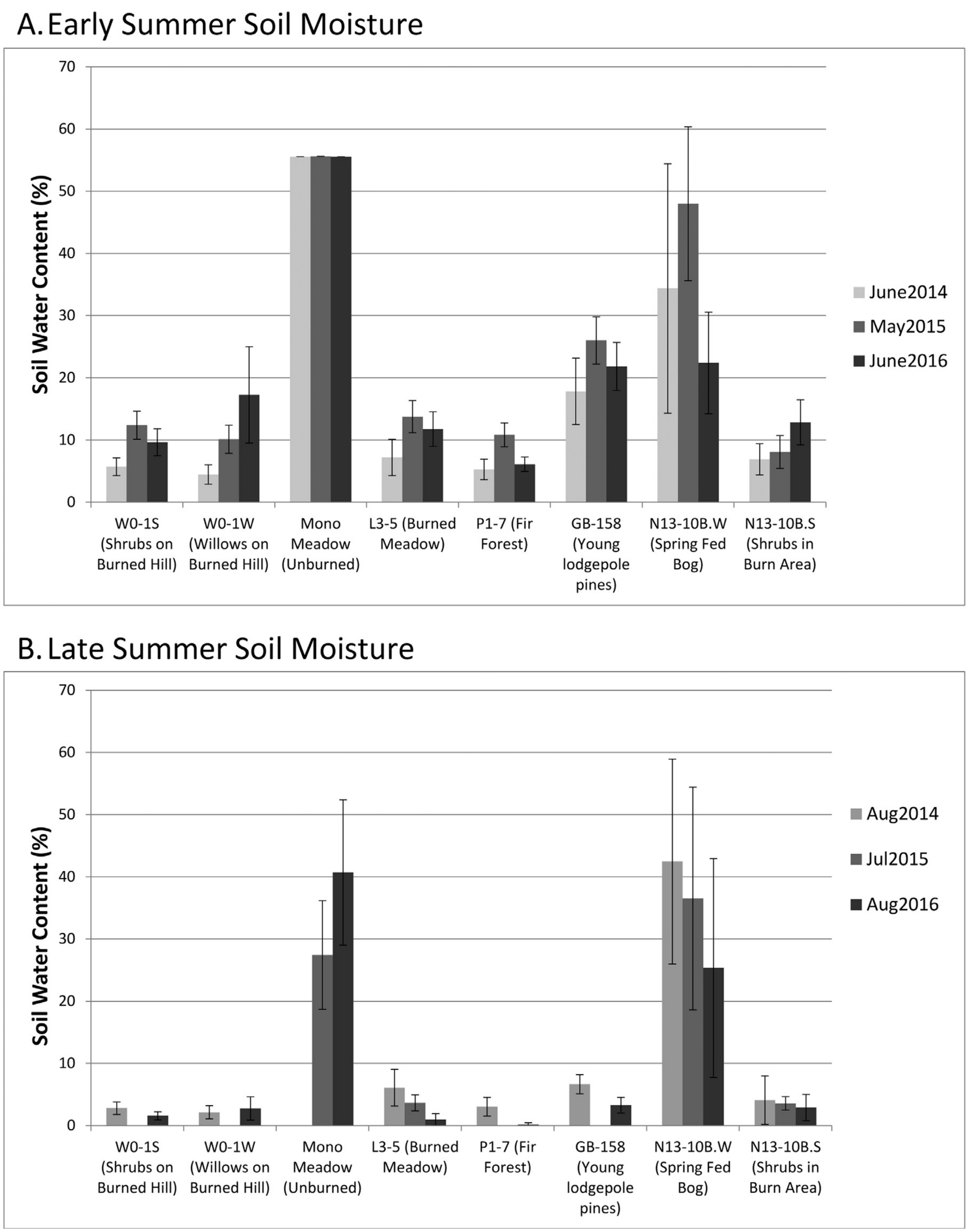

Fig. D.1. Mean volumetric soil water content (as a %) for a subset of sites spanning a range of fire histories and land cover for May–June (A) and July–August (B). Some sites are missing one year of July–August data (a missing bar does not indicate a value of 0). Error bars denote standard deviations.

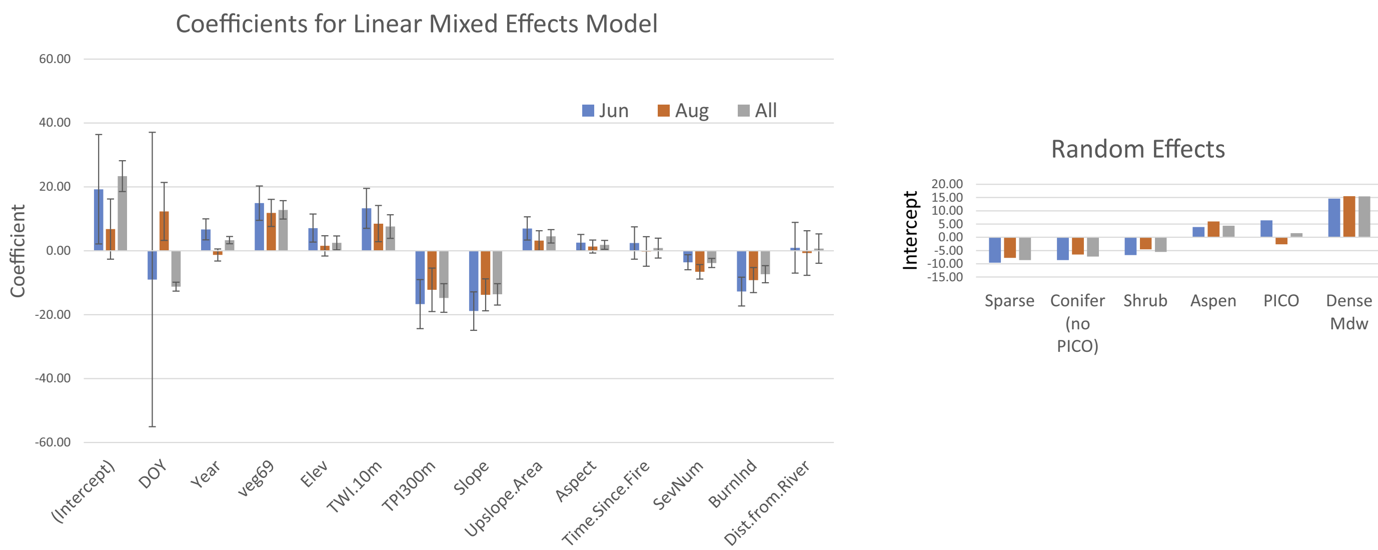

Fig. D.2. Model coefficients vary depending on time of year. This plot shows the fixed effect coefficients and random effect intercepts from using the linear model. The results are shown separately for models trained on early summer data only (blue), late summer only (orange) and all data. (For interpretation of the references to color in this figure legend, the reader is referred to the web version of this article.)

(Figs. C.1 and D.1). For this reason, we explored the option of creating separate model fits for early summer (prior to July 15) and late summer (after July 15). For most model coefficients, there were not significant differences between fitting data from the two different time periods (Fig. D.2).

A formal definition of *partial dependence* for random forest models is provided here for clarification:

Define a model $f(X)$, where X contains p covariates $\mathbf{x_j}$ with n observations each. An individual value within $\mathbf{x_j}$ is given by $x_{j,\,k}$, $j = 1.\,.p$, $k = 1.\,.n$. The partial dependence, $\widetilde{f}\,(x_{j,k})$, of an individual covariate value $x_{j,\,k}$ is found by taking the average value of f using the given $x_{j,\,k}$ across all possible values for the other covariates:

$$\widetilde{f}\,(x_{j,k}) = \frac{1}{n}\sum_{i=1}^{n} f\,(x_{1,i},\,\ldots,x_{j-1,i},\,x_{j,k},\,x_{j+1,i},\,\ldots,x_{p,i}) \tag{D.1}$$

Calculating $\widetilde{f}\,(x_{j,k})$ for $k = 1.\,.n$ gives a plot of the mean value of $f(X)$ for a given value of $\mathbf{x_j}$, or the partial dependence of f on $\mathbf{x_j}$.

Appendix E. Deeper soil moisture

The soil moisture data in Appendix C suggests that the difference between shallow and deep soil moisture is greater in shrubs and wetlands than it is in closed-canopy forests. This could mean that soil moisture changes resulting from conifer removal may be greater at depth than in surface soil (top 12 cm). As a preliminary exercise to test the significance of this, we extrapolated the 0–1 m depth-averaged soil moisture values from the weather stations to the full watershed using vegetation maps. We assumed that the relationship between shallow and deep soil moisture fits a separate linear equation for each vegetation type:

$$(\text{Mean VWC over top 1m}) = C_{1,v} + C_{2,v} \times (\text{Mean VWC over top 12 cm})$$

where $C_{1,\,v}$ and $C_{2,\,v}$ are coefficients unique to each vegetation type, v. The stationarity of these coefficients over time and space cannot be verified given the limited number of deep VWC measurements available. However, further work using additional buried sensors and/or hydrologic models may validate this estimate.

Using summer soil moisture data from the three weather stations, we calculated the coefficients given in Table E.1.

Applying the appropriate linear equation to the surface soil moisture estimates in each grid cell of our basin-scale model gives an estimated 1-meter averaged soil moisture value. We used the coefficients for shrub to estimate soil moisture for sparse meadows, under the assumption that sparse meadows and shrublands both have relatively shallow-rooted vegetation, and that sparse meadow moisture regimes are likely more similar to shrublands than they are to wet meadows. The results of this exercise showed a 7% increase in soil moisture across the whole watershed under 2014 conditions compared to if the watershed had remained fire suppressed. For comparison, the model of surface soil moisture showed a 2% decrease in surface soil moisture averaged across the basin.

Table E.1
Linear model coefficients relating soil moisture averaged across the top meter of soil to moisture in the top 12 cm only.

Veg. Type	$C_{1,\,v}$	$C_{2,\,v}$
Forest	0.0	1.2
Shrub	0.0	1.9
Dense Meadow	0.2	0.5

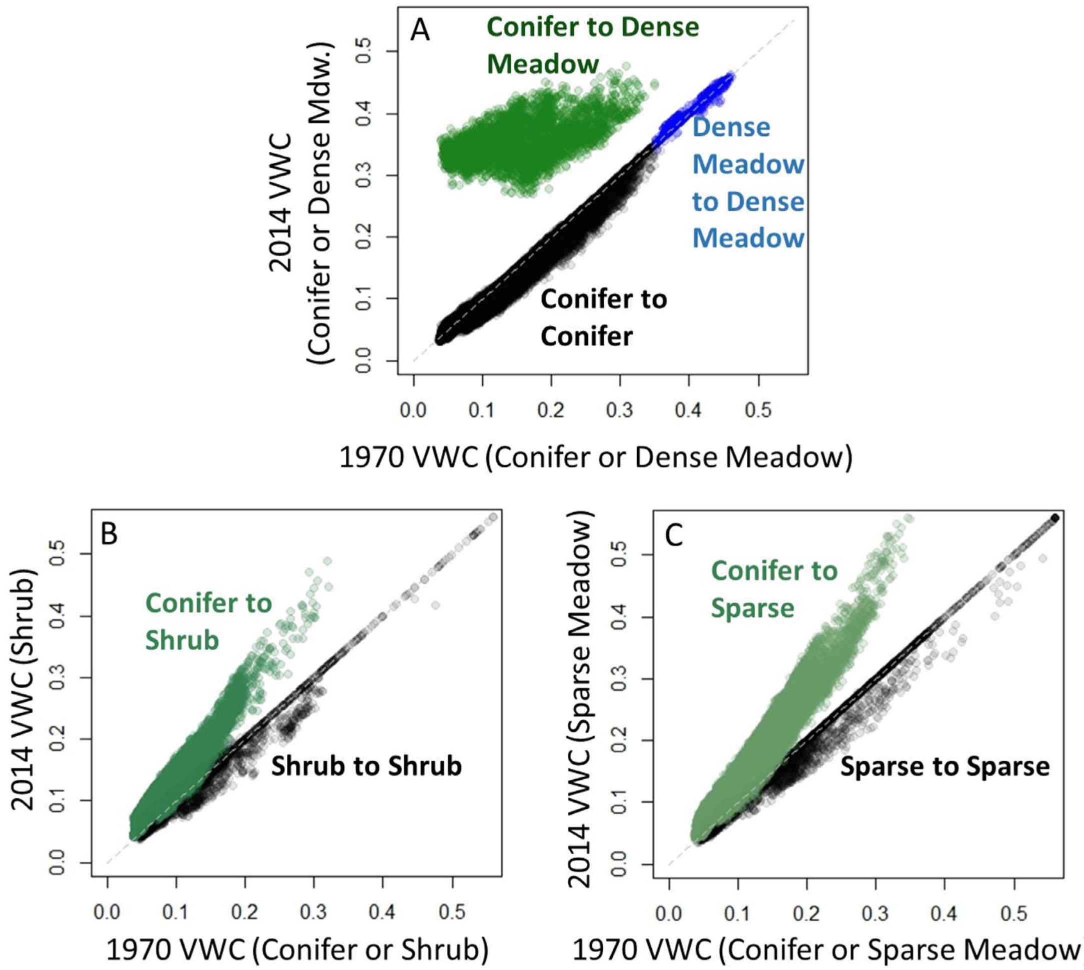

Fig. E.1. Modeled VWC over the top meter of soil under different types of vegetation transitions. A: Conifer-dominated in both time periods (black), dense meadow in both time periods (blue), or locations that transitioned from conifer to dense meadow (green). B: Locations that were either shrub in both 1970 and 2014 (black) or transitioned from conifer to shrub (green). C: Locations that were either sparse meadow in both 1970 and 2014 (black) or transitioned from conifer to sparse meadow (green). (For interpretation of the references to color in this figure legend, the reader is referred to the web version of this article.)

This increase in mean soil moisture for the top meter is mainly driven by a large increase in deep soil moisture under the drier dense meadows (Fig. E.1(A)) compared to the smaller increases in surface soil moisture alone for the same vegetation transitions (Fig. E.2(A)). There are also slight increases in soil moisture over the top meter when transitioning from conifer to shrubs or sparse meadow (Fig. E.1(B) and (C)), with the largest changes occurring in areas that were already at the wetter end of the range. For comparison, surface soil moisture was predicted to change very little or slightly decrease under transitions from conifer to shrubs or sparse meadows (Fig. E.2(B) and (C)).

Because we only have one location with deep soil moisture measurements under each vegetation type, these estimates of change in deeper soil moisture are highly uncertain. However, this analysis does illustrate the possibility that transitions from conifer to other vegetation types could increase total soil water stores to a greater degree than is observed using surface soil moisture alone.

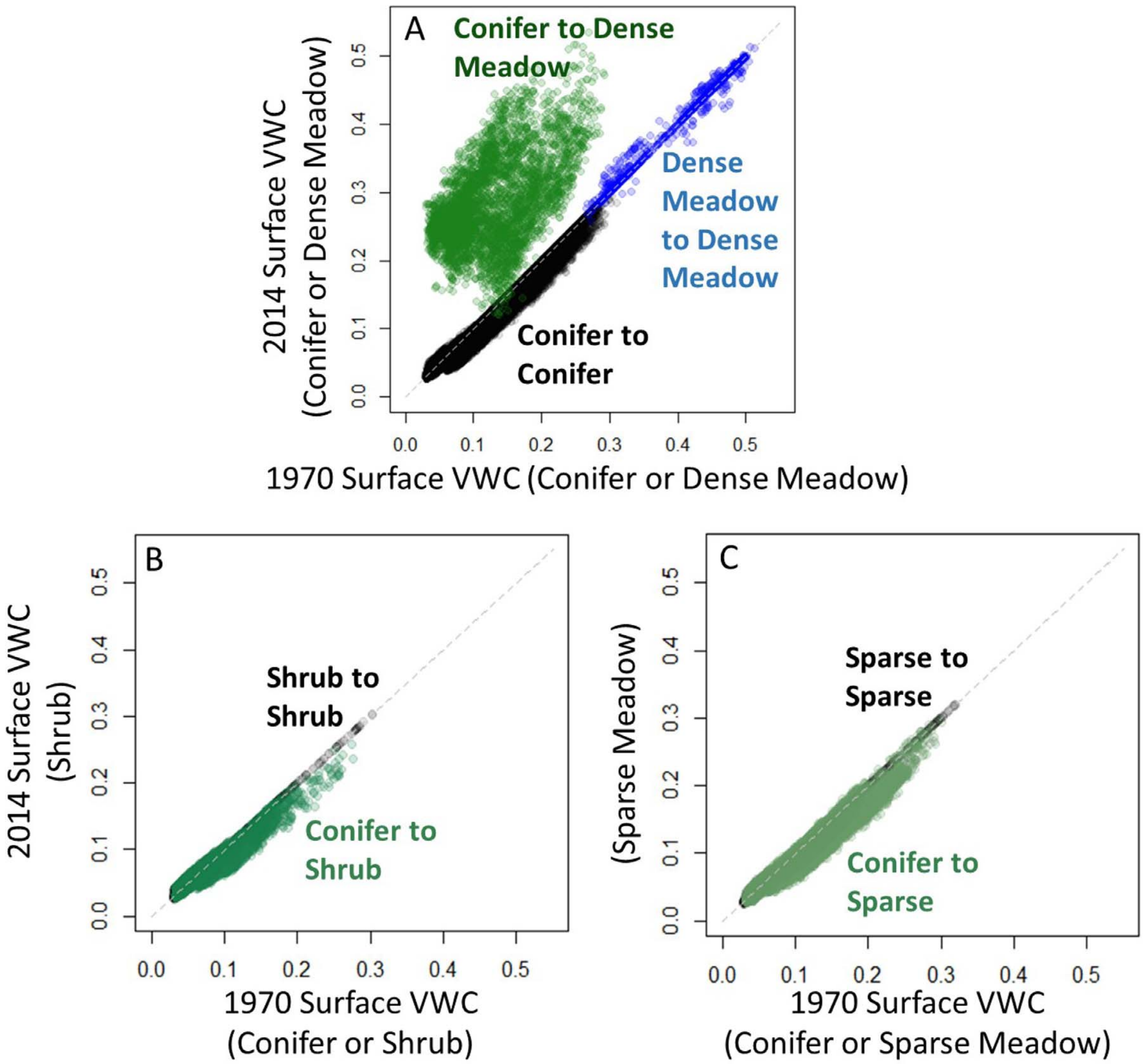

Fig. E.2. Modeled VWC over the top 12cm of soil under different types of vegetation transitions. A: Conifer-dominated in both time periods (black), dense meadow in both time periods (blue), or locations that transitioned from conifer to dense meadow (green). B: Locations that were either shrub in both 1970 and 2014 (black) or transitioned from conifer to shrub (green). C: Locations that were either sparse meadow in both 1970 and 2014 (black) or transitioned from conifer to sparse meadow (green). (For interpretation of the references to color in this figure legend, the reader is referred to the web version of this article.)

References

Araya, Y.N., Silvertown, J., Gowing, D.J., McConway, K.J., Peter Linder, H., Midgley, G., 2011. A fundamental, eco-hydrological basis for niche segregation in plant communities. New Phytol. 189 (1), 253–258. http://dx.doi.org/10.1111/j.1469-8137.2010.03475.x.

Aust, W.M., Blinn, C.R., 2004. Forestry best management practices for timber harvesting and site preparation in the eastern United States: An overview of water quality and productivity research during the past 20 years (1982–2002). Water, Air Soil Pollut. 4 (1), 5–36. http://dx.doi.org/10.1023/B:WAFO.0000012828.33069.f6.

Baker, M.B., 1986. Effects of ponderosa pine treatments on water yield in Arizona. Water Resour. Res. 22 (1), 67–73. http://dx.doi.org/10.1029/WR022i001p00067.

Bales, R.C., Hopmans, J.W., O'Geen, A.T., Meadows, M., Hartsough, P.C., Kirchner, P., Hunsaker, C.T., Beaudette, D., 2011. Soil moisture response to snowmelt and rainfall in a Sierra Nevada mixed-conifer forest. Vadose Zone J. 10 (3), 786–799.

Beven, K., 1983. Surface water hydrologyrunoff generation and basin structure. Rev. Geophys. 21 (3), 721–730. http://dx.doi.org/10.1029/RG021i003p00721.

Biederman, J., Harpold, A., Gochis, D., Ewers, B., Reed, D., Papuga, S., Brooks, P., 2014. Increased evaporation following widespread tree mortality limits streamflow response. Water Resour. Res. 50 (7), 5395–5409. http://dx.doi.org/10.1002/2013WR014994.

Boisramé, G., Thompson, S., Collins, B., Stephens, S., 2017. Managed wildfire effects on forest resilience and water in the sierra nevada. Ecosystems 20 (4), 717–732. http://dx.doi.org/10.1007/s10021-016-0048-1.

Boisramé, G.F., Thompson, S.E., Kelly, M., Cavalli, J., Wilkin, K.M., Stephens, S.L., 2017. Vegetation change during 40 years of repeated managed wildfires in the Sierra Nevada, California. For. Ecol. Manag. 402, 241–252. http://dx.doi.org/10.1016/j.foreco.2017.07.034.

Bréda, N., Granier, A., Aussenac, G., 1995. Effects of thinning on soil and tree water relations, transpiration and growth in an oak forest (quercus petraea (matt.) liebl.). Tree Physiol. 15 (5), 295–306.

Bréda, N., Granier, A., Barataud, F., Moyne, C., 1995. Soil water dynamics in an oak stand. Plant Soil 172 (1), 17–27. http://dx.doi.org/10.1007/BF00020856.

Breiman, L., 2001. Random forests. Mach. Learn. 45 (1), 5–32. http://dx.doi.org/10.1023/A:1010933404324.

Brown, A.E., Zhang, L., McMahon, T.A., Western, A.W., Vertessy, R.A., 2005. A review of paired catchment studies for determining changes in water yield resulting from alterations in vegetation. J. Hydrol. 310 (14), 28–61. http://dx.doi.org/10.1016/j.jhydrol.2004.12.010.

Campbell Scientific, 2015. HS2. http://www.campbellsci.com/hs2.

Chan, S.K., Bindlish, R., O'Neill, P.E., Njoku, E., Jackson, T., Colliander, A., Chen, F., Burgin, M., Dunbar, S., Piepmeier, J., Yueh, S., Entekhabi, D., Cosh, M.H., Caldwell, T., Walker, J., Wu, X., Berg, A., Rowlandson, T., Pacheco, A., McNairn, H., Thibeault, M., Martinez-Fernandez, J., Gonzalez-Zamora, A., Seyfried, M., Bosch, D., Starks, P., Goodrich, D., Prueger, J., Palecki, M., Small, E.E., Zreda, M., Calvet, J.C., Crow, W.T., Kerr, Y., 2016. Assessment of the SMAP passive soil moisture product. IEEE Trans. Geosci. Remote Sens. 54 (8), 4994–5007. http://dx.doi.org/10.1109/TGRS.2016.2561938.

Chen, Q., Laurin, G.V., Battles, J.J., Saah, D., 2012. Integration of airborne lidar and vegetation types derived from aerial photography for mapping aboveground live biomass. Remote Sens. Environ. 121, 108–117. http://dx.doi.org/10.1016/j.rse.2012.01.021.

Clark, J., 2007. Models for Ecological Data. Princeton University Press, Princeton.

Collins, B., Kelly, M., van Wagtendonk, J., Stephens, S., 2007. Spatial patterns of large natural fires in Sierra Nevada wilderness areas. Landsc. Ecol. 22 (4), 545–557. http://dx.doi.org/10.1007/s10980-006-9047-5.
Collins, B., Miller, J., Thode, A., Kelly, M., van Wagtendonk, J., Stephens, S., 2009. Interactions among wildland fires in a long-established Sierra Nevada natural fire area. Ecosystems 12, 114–128. http://dx.doi.org/10.1007/s10021-008-9211-7.
Collins, B.M., Everett, R.G., Stephens, S.L., 2011. Impacts of fire exclusion and recent managed fire on forest structure in old growth Sierra Nevada mixed-conifer forests. Ecosphere 2 (4), 1–14. http://dx.doi.org/10.1890/ES11-00026.1.
Collins, B.M., Lydersen, J.M., Fry, D.L., Wilkin, K., Moody, T., Stephens, S.L., 2016. Variability in vegetation and surface fuels across mixed-conifer-dominated landscapes with over 40 years of natural fire. For. Ecol. Manag. 381, 74–83. http://dx.doi.org/10.1016/j.foreco.2016.09.010.
Collins, B.M., Stephens, S.L., 2007. Managing natural wildfires in Sierra Nevada wilderness areas. Front. Ecol. Environ. 5 (10), 523–527. http://dx.doi.org/10.1890/070007.
Collins, B.M., Stephens, S.L., 2010. Stand-replacing patches within a 'mixed severity' fire regime: quantitative characterization using recent fires in a long-established natural fire area. Landsc. Ecol. 25 (6), 927–939. http://dx.doi.org/10.1007/s10980-010-9470-5.
Crist, E.P., Cicone, R.C., 1984. A physically-based transformation of thematic mapper data—the TM Tasseled Cap. Geosci. Remote Sens. IEEE Trans. 22 (3), 256–263.
Dawson, T.E., Burgess, S.S.O., Tu, K.P., Oliveira, R.S., Santiago, L.S., Fisher, J.B., Simonin, K.A., Ambrose, A.R., 2007. Nighttime transpiration in woody plants from contrasting ecosystems. Tree Physiol. 27 (4), 561–575. http://dx.doi.org/10.1093/treephys/27.4.561.
Dawson, T.E., Ehleringer, J.R., 1993. Gender-specific physiology, carbon isotope discrimination, and habitat distribution in Boxelder, Acer Negundo. Ecology 74 (3), 798–815. http://dx.doi.org/10.2307/1940807.
Dettinger, M.D., Anderson, M.L., 2015. Storage in California's reservoirs and snowpack in this time of drought. San Franc. Estuary Watershed Sci. 13 (2), 1–5. http://dx.doi.org/10.15447/sfews.2015v13iss2art1.
Dormann, C.F., Elith, J., Bacher, S., Buchmann, C., Carl, G., Carre, G., Marquez, J.R.G., Gruber, B., Lafourcade, B., Leitao, P.J., Munkemuller, T., McClean, C., Osborne, P.E., Reineking, B., Schroder, B., Skidmore, A.K., Zurell, D., Lautenbach, S., 2013. Collinearity: a review of methods to deal with it and a simulation study evaluating their performance. Ecography 36 (1), 27–46. http://dx.doi.org/10.1111/j.1600-0587.2012.07348.x.
Dubé, S., Plamondon, A.P., Rothwell, R.L., 1995. Watering up after clear-cutting on forested wetlands of the st. lawrence lowland. Water Resour. Res. 31 (7), 1741–1750. http://dx.doi.org/10.1029/95WR00427.
Ellis, C.R., Pomeroy, J.W., Link, T.E., 2013. Modeling increases in snowmelt yield and desynchronization resulting from forest gap-thinning treatments in a northern mountain headwater basin. Water Resour. Res. 49 (2), 936–949. http://dx.doi.org/10.1002/wrcr.20089.
Famiglietti, J.S., Ryu, D., Berg, A.A., Rodell, M., Jackson, T.J., 2008. Field observations of soil moisture variability across scales. Water Resour. Res. 44 (1). http://dx.doi.org/10.1029/2006WR005804. W01423.
Fites-Kaufman, J.A., Rundel, P., Stephenson, N., Weixelman, D.A., 2007. Montane and subalpine vegetation of the Sierra Nevada and Cascade ranges. Terrestrial Vegetation of California. University of California Press, Berkeley, pp. 456–501.
Fletcher, M.-S., Wood, S.W., Haberle, S.G., 2014. A fire-driven shift from forest to non-forest: evidence for alternative stable states? Ecology 95 (9), 2504–2513. http://dx.doi.org/10.1890/12-1766.1.
Gonzalez-Zamora, A., Sanchez, N., Martinez-Fernandez, J., Wagner, W., 2016. Root-zone plant available water estimation using the smos-derived soil water index. Adv. water resour. 96, 339–353. http://dx.doi.org/10.1016/j.advwatres.2016.08.001.
Grant, G.E., Tague, C.L., Allen, C.D., 2013. Watering the forest for the trees: an emerging priority for managing water in forest landscapes. Front. Ecol. Environ. 11 (6), 314–321. http://dx.doi.org/10.1890/120209.
Grayson, R.B., Western, A.W., Chiew, F.H., Blņschl, G., 1997. Preferred states in spatial soil moisture patterns: local and nonlocal controls. Water Resour. Res. 33 (12), 2897–2908. http://dx.doi.org/10.1029/97WR02174.
Griffin, D., Anchukaitis, K.J., 2014. How unusual is the 2012 - 2014 California drought? Geophys. Res. Lett. 41 (24), 9017–9023. http://dx.doi.org/10.1002/2014GL062433. 2014GL062433.
Grömping, U., 2009. Variable importance assessment in regression: linear regression versus random forest. Am. Stat. 63 (4), 308–319. http://dx.doi.org/10.1198/tast.2009.08199.
Hawthorne, S.N., Lane, P.N., Bren, L.J., Sims, N.C., 2013. The long term effects of thinning treatments on vegetation structure and water yield. For. Ecol. Manag. 310 (Supplement C), 983–993. http://dx.doi.org/10.1016/j.foreco.2013.09.046.
He, L., Ivanov, V.Y., Bohrer, G., Thomsen, J.E., Vogel, C.S., Moghaddam, M., 2013. Temporal dynamics of soil moisture in a northern temperate mixed successional forest after a prescribed intermediate disturbance. Agric. For. Meteorol. 180 (0), 22–33. http://dx.doi.org/10.1016/j.agrformet.2013.04.014.
Helms, J.A., 1987. Invasion of Pinus contorta var. murrayana (pinaceae) into mountain meadows at Yosemite National Park, California. MadroŞo 34 (2), 91–97.
Helms, J.A., Ratliff, R.D., 1987. Germination and establishment of Pinus contorta var. murrayana (pinaceae) in mountain meadows of Yosemite National Park, California. Madroño 34 (2), 77–90.
Helvey, J., 1980. Effects of a north central Washington wildfire on runoff and sediment production. Water Resour. Bull. 16 (4), 627–634.
Hibbert, A.R., 1965. Forest Treatment Effects on Water Yield. Citeseer.
Kane, V.R., Lutz, J.A., Alina Cansler, C., Povak, N.A., Churchill, D.J., Smith, D.F., Kane, J.T., North, M.P., 2015. Water balance and topography predict fire and forest structure patterns. For. Ecol. Manag. 338, 1–13. http://dx.doi.org/10.1016/j.foreco.2014.10.038.
Kane, V.R., North, M.P., Lutz, J.A., Churchill, D.J., Roberts, S.L., Smith, D.F., McGaughey, R.J., Kane, J.T., Brooks, M.L., 2014. Assessing fire effects on forest spatial structure using a fusion of Landsat and airborne LiDAR data in Yosemite National Park. Remote Sens. Environ. 151, 89–101. http://dx.doi.org/10.1016/j.rse.2013.07.041.
Kattelmann, R.C., Berg, N.H., Rector, J., 1983. The potential for increasing streamflow from Sierra Nevada watersheds. JAWRA J. Am. Water Resour.Assoc. 19 (3), 395–402. http://dx.doi.org/10.1111/j.1752-1688.1983.tb04596.x.
Kauffman, J.B., 2004. Death rides the forest: perceptions of fire, land use, and ecological restoration of western forests. Conserv. Biol. 18 (4), 878–882. http://dx.doi.org/10.1111/j.1523-1739.2004.545_1.x.
Lane, P., Feikema, P., Sherwin, C., Peel, M., Freebairn, A., 2010. Modelling the long term water yield impact of wildfire and other forest disturbance in eucalypt forests. Environ. Model. Softw. 25 (4), 467–478. http://dx.doi.org/10.1016/j.envsoft.2009.11.001.
Langford, K., 1976. Change in yield of water following a bushfire in a forest of eucalyptus regnans. J. Hydrol. 29 (1), 87–114.
Lesch, W., Scott, D.F., 1997. The response in water yield to the thinning of Pinus radiata, Pinus patula and Eucalyptus grandis plantations. For. Ecol. Manag. 99 (3), 295–307. http://dx.doi.org/10.1016/S0378-1127(97)00045-5.
Liaw, A., Wiener, M., 2002. Classification and regression by randomforest. R News 2 (3), 18–22.
Lowry, C.S., Loheide, S.P., Moore, C.E., Lundquist, J.D., 2011. Groundwater controls on vegetation composition and patterning in mountain meadows. Water Resour. Res. 47 (10), W00J11. http://dx.doi.org/10.1029/2010WR010086.
Lundquist, J.D., Dickerson-Lange, S.E., Lutz, J.A., Cristea, N.C., 2013. Lower forest density enhances snow retention in regions with warmer winters: a global framework developed from plot-scale observations and modeling. Water Resour. Res. 49 (10), 6356–6370. http://dx.doi.org/10.1002/wrcr.20504.
Ma, S., Concilio, A., Oakley, B., North, M., Chen, J., 2010. Spatial variability in microclimate in a mixed-conifer forest before and after thinning and burning treatments. For. Ecol. Manag. 259 (5), 904–915. http://dx.doi.org/10.1016/j.foreco.2009.11.030.
McIntyre, P.J., Thorne, J.H., Dolanc, C.R., Flint, A.L., Flint, L.E., Kelly, M., Ackerly, D.D., 2015. Twentieth-century shifts in forest structure in California: denser forests, smaller trees, and increased dominance of oaks. Proc. Nat.l Acad. Sci. 112 (5), 1458–1463. http://dx.doi.org/10.1073/pnas.1410186112.
McLaughlin, B.C., Ackerly, D.D., Klos, P.Z., Natali, J., Dawson, T.E., Thompson, S.E., 2017. Hydrologic refugia, plants, and climate change. Glob. Change Biol. 23 (8), 2941–2961. http://dx.doi.org/10.1111/gcb.13629.
Milledge, D.G., Warburton, J., N. Lane, S., J. Stevens, C., 2013. Testing the influence of topography and material properties on catchment-scale soil moisture patterns using remotely sensed vegetation patterns in a humid temperate catchment, northern Britain. Hydrol. Process. 27 (8), 1223–1237. http://dx.doi.org/10.1002/hyp.9292.
Miller, J.D., Thode, A.E., 2007. Quantifying burn severity in a heterogeneous landscape with a relative version of the delta Normalized Burn Ratio (dNBR). Remote Sens. Environ. 109 (1), 66–80. http://dx.doi.org/10.1016/j.rse.2006.12.006.
Mountford, J., Chapman, J., 1993. Water regime requirements of British wetland vegetation: using the moisture classification of Ellenberg and Londo. J. Environ. Manag. 38 (4), 275–288. http://dx.doi.org/10.1006/jema.1993.1045.
Musick, H., Pelletier, R.E., 1988. Response to soil moisture of spectral indexes derived from bidirectional reflectance in thematic mapper wavebands. Remote Sens. Environ. 25 (2), 167–184. http://dx.doi.org/10.1016/0034-4257(88)90099-5.
Neary, D., Ryan, K.C., DeBano, L.F., 2005. Wildland Fire in Ecosystems: Effects of Fire on Soil and Water. Technical Report. United States Department of Agriculture. Forest Service.
Norman, S.P., Taylor, A.H., 2005. Pine forest expansion along a forest-meadow ecotone in northeastern California, USA. For. Ecol. Manag. 215 (13), 51–68. http://dx.doi.org/10.1016/j.foreco.2005.05.003.
Omuto, C., Vargas, R., Alim, M., Paron, P., 2010. Mixed-effects modelling of time series NDVI-rainfall relationship for detecting human-induced loss of vegetation cover in drylands. J. Arid Environ. 74 (11), 1552–1563. http://dx.doi.org/10.1016/j.jaridenv.2010.04.001.
Pinheiro, J., Bates, D., DebRoy, S., Sarkar, D., R Core Team, 2015. nlme: linear and nonlinear mixed effects models. R package version 3.1-122.
Pollet, J., Omi, P.N., 2002. Effect of thinning and prescribed burning on crown fire severity in ponderosa pine forests. Int. J. Wildland Fire 11 (1), 1–10. http://dx.doi.org/10.1071/WF01045.
Ponisio, L.C., Wilkin, K., M'Gonigle, L.K., Kulhanek, K., Cook, L., Thorp, R., Griswold, T., Kremen, C., 2016. Pyrodiversity begets plant-pollinator community diversity. Glob. Change Biol. 22 (5), 1794–1808. http://dx.doi.org/10.1111/gcb.13236.
Prasad, A.M., Iverson, L.R., Liaw, A., 2006. Newer classification and regression tree techniques: bagging and random forests for ecological prediction. Ecosystems 9 (2), 181–199. http://dx.doi.org/10.1007/s10021-005-0054-1.
Rambo, T., North, M., 2009. Canopy microclimate response to pattern and density of thinning in a Sierra Nevada forest. For. Ecol. Manag. 257 (2), 435–442.
Ratliff, R.D., 1985. Meadows in the Sierra Nevada of California: state of knowledge. Technical Report. Pacific Southwest Forest and Range Experiment Station, Forest Service, U.S. Department of Agriculture.
Ridolfi, L., D'Odorico, P., Laio, F., 2006. Effect of vegetation water table feedbacks on the stability and resilience of plant ecosystems. Water Resour. Res. 42 (1), n/a–n/a. http://dx.doi.org/10.1029/2005WR004444. W01201.
Rodriguez-Iturbe, I., D'Odorico, P., Laio, F., Ridolfi, L., Tamea, S., 2007. Challenges in humid land ecohydrology: interactions of water table and unsaturated zone with climate, soil, and vegetation. Water Resour. Res. 43 (9), W09301. http://dx.doi.org/

10.1029/2007WR006073.
Roth, C.H., Malicki, M.A., Plagge, R., 1992. Empirical evaluation of the relationship between soil dielectric constant and volumetric water content as the basis for calibrating soil moisture measurements by TDR. J. Soil Sci. 43 (1), 1–13. http://dx.doi.org/10.1111/j.1365-2389.1992.tb00115.x.
Royce, E.B., Barbour, M.G., 2001. Mediterranean climate effects. I. Conifer water use across a Sierra Nevada ecotone. Am. J. Bot. 88 (5), 911–918. arXiv: http://www.amjbot.org/content/88/5/911.full.pdf+html.
Ruprecht, J., Stoneman, G., 1993. Water yield issues in the jarrah forest of south-western Australia. J. Hydrol. 150 (2), 369–391. http://dx.doi.org/10.1016/0022-1694(93)90117-R.
Sellin, A., 1999. Does pre-dawn water potential reflect conditions of equilibrium in plant and soil water status? Acta Oecol. 20 (1), 51–59. http://dx.doi.org/10.1016/S1146-609X(99)80015-0.
Shmueli, G., 2010. To explain or to predict? Statist. Sci. 25 (3), 289–310. http://dx.doi.org/10.1214/10-STS330.
Sörensen, R., Zinko, U., Seibert, J., 2006. On the calculation of the topographic wetness index: evaluation of different methods based on field observations. Hydrol. Earth Syst. Sci. Discuss. 10 (1), 101–112.
Stephens, S.L., Moghaddas, J.J., Edminster, C., Fiedler, C.E., Haase, S., Harrington, M., Keeley, J.E., Knapp, E.E., McIver, J.D., Metlen, K., Skinner, C.N., Youngblood, A., 2009. Fire treatment effects on vegetation structure, fuels, and potential fire severity in western U.S. forests. Ecol. Appl. 19 (2), 305–320. http://dx.doi.org/10.1890/07-1755.1.
Tague, C., Dugger, A.L., 2010. Ecohydrology and climate change in the mountains of the western USA - a review of research and opportunities. Geogr. Compass 4 (11), 1648–1663. http://dx.doi.org/10.1111/j.1749-8198.2010.00400.x.
Troendle, C.A., 1983. The potential for water yield augmentation from forest management in the rocky mountain region. J. Am. Water Resour. Assoc. 19, 359–373. http://dx.doi.org/10.1111/j.1752-1688.1983.tb04593.x.
UCLA: Statistical Consulting Group, 2017. R library contrast coding systems for categorical variables. http://stats.idre.ucla.edu/r/library/r-library-contrast-coding-systems-for-categorical-variables/.
U.S. Congress, 1964. The wilderness act: public law 88-577 (16 U.S. C. 1131-1136). http://wilderness.nps.gov/document/wildernessAct.pdf.
Vertessy, R., Benyon, R., O'sullivan, S., Gribben, P., 1995. Relationships between stem diameter, sapwood area, leaf area and transpiration in a young mountain ash forest. Tree Physiol. 15 (9), 559–567. http://dx.doi.org/10.1093/treephys/15.9.559.
Vertessy, R.A., Watson, F.G., Sharon, K., et al., 2001. Factors determining relations between stand age and catchment water balance in mountain ash forests. Forest Ecol. Manag. 143 (1), 13–26. http://dx.doi.org/10.1016/S0378-1127(00)00501-6.
van Wagtendonk, J.W., 2007. The history and evolution of wildland fire use. Fire Ecol. 3, 3–17. http://dx.doi.org/10.4996/fireecology.0302003.
Weiss, A., 2001. Topographic position and landforms analysis. Poster presentation, ESRI User Conference, San Diego, CA. 200–200.
Western, A.W., Blöschl, G., Grayson, R.B., 1998. Geostatistical characterisation of soil moisture patterns in the Tarrawarra catchment. J. Hydrol. 205 (142), 20–37. http://dx.doi.org/10.1016/S0022-1694(97)00142-X.
Western, A.W., Grayson, R.B., Blöschl, G., Willgoose, G.R., McMahon, T.A., 1999. Observed spatial organization of soil moisture and its relation to terrain indices. Water Resour. Res. 35 (3), 797–810. http://dx.doi.org/10.1029/1998WR900065.
Zhang, L., Dawes, W.R., Walker, G.R., 2001. Response of mean annual evapotranspiration to vegetation changes at catchment scale. Water Resour. Res. 37 (3), 701–708. http://dx.doi.org/10.1029/2000WR900325.